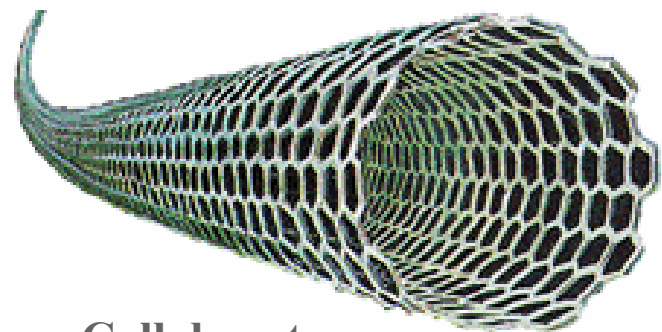


Tutorial on Physical Properties and Characterization of Carbon Nanotubes

Mildred Dresselhaus

Massachusetts Institute of Technology

Cambridge, MA



Collaborators:

G. Dresselhaus, MIT

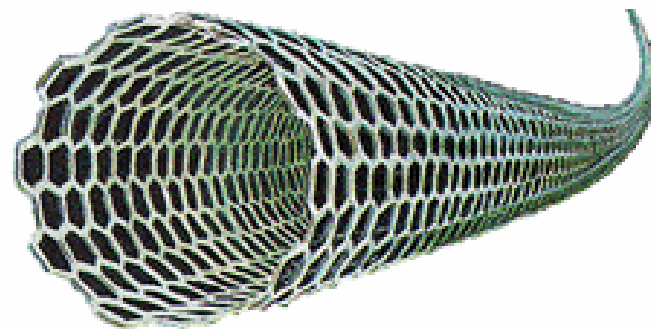
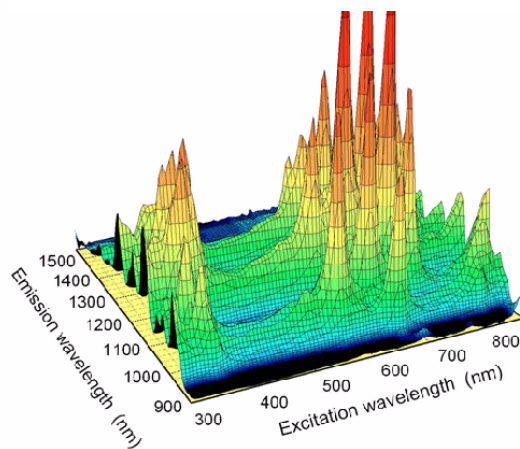
G. Samsonidze, MIT

G. Chou, MIT

H. Son, MIT

M. Zhang, DuPont

M. Terrones, Mexico



Collaborators:

A. Souza, Brazil

A. Jorio, Brazil

M.A. Pimenta, Brazil

J. Jiang, Japan

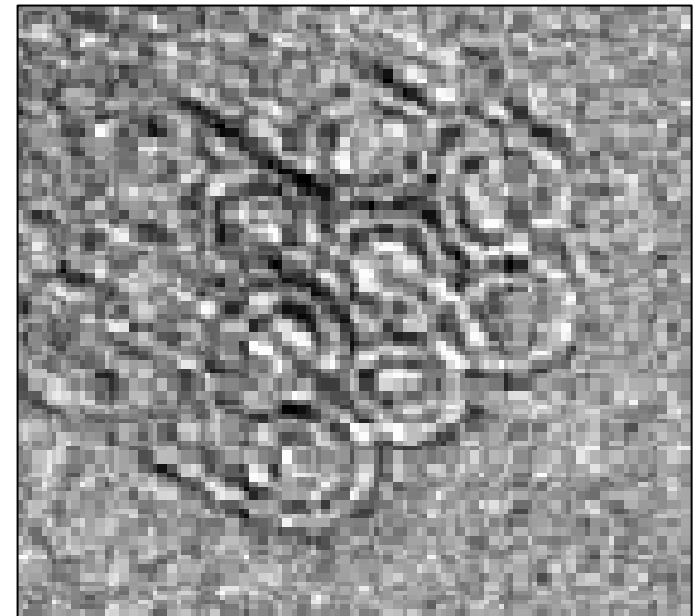
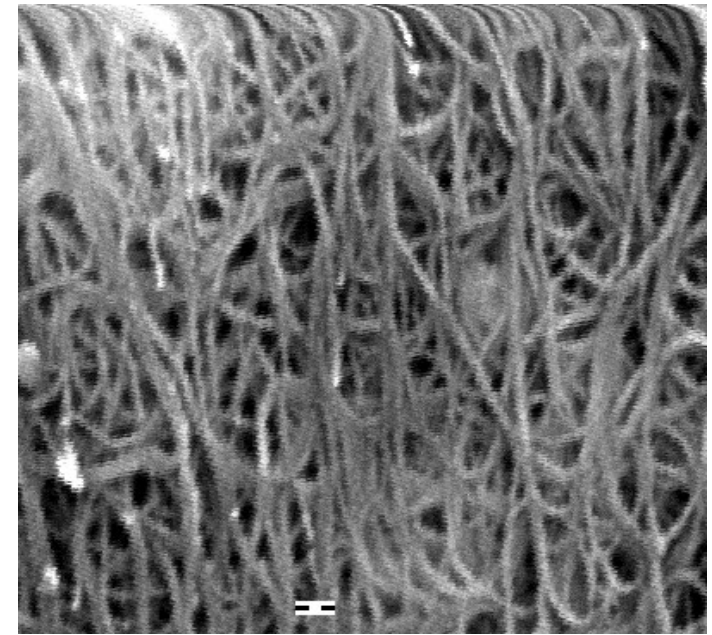
R. Saito, Japan

M. Endo, Japan

Outline on Characterization with a Focus on optical characterization

- **What is in my sample?**
- **What we can learn from:**
 - **Photoluminescence?**
 - **Raman spectroscopy?**
 - **Fast Optics?**

Sample characterization by SEM and TEM

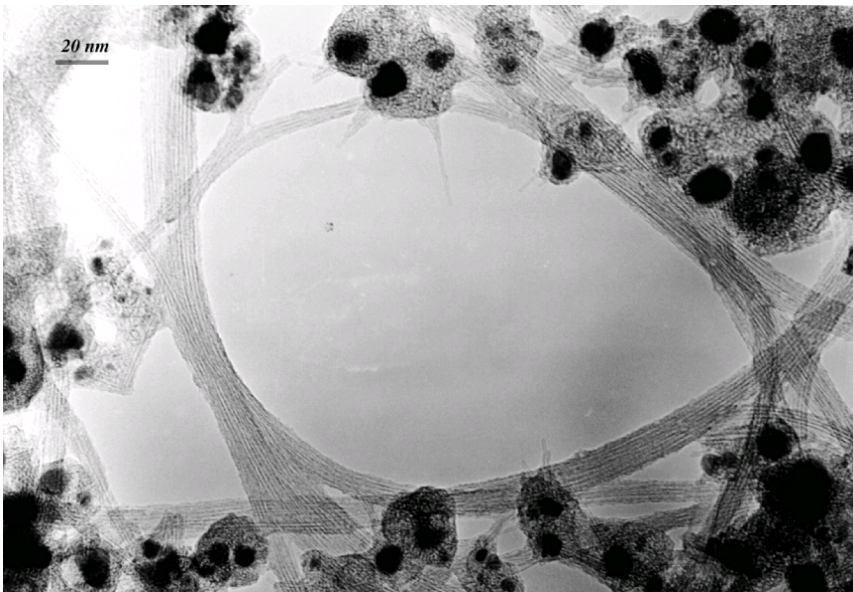


Bundles of double wall carbon nanotubes produced at **UFMG** by the electric arc method and characterized by SEM and TEM

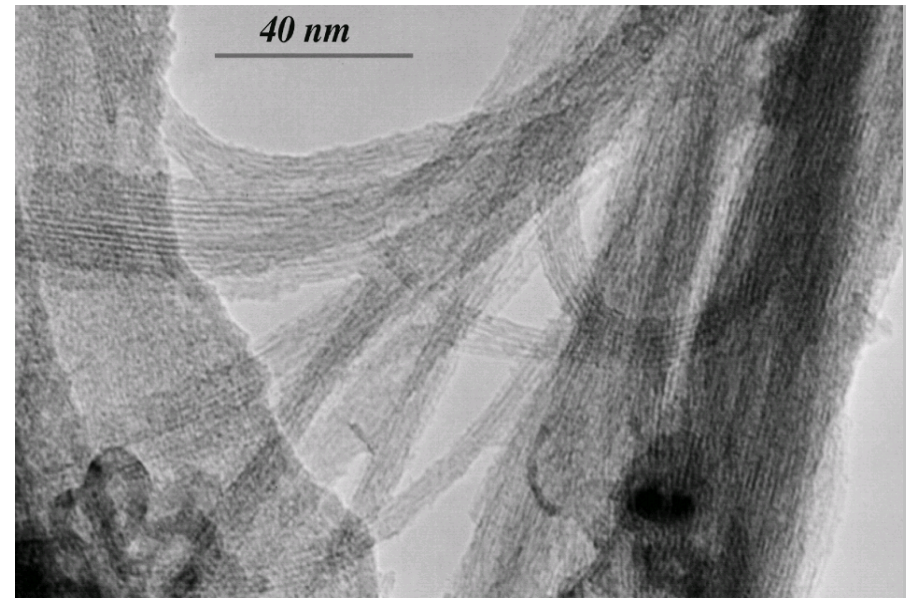
TEM for characterization of the purification process

TEM: characterizes the overall structure of nanotube samples showing catalyst particles and nanotube ropes.

Before purification : 30% of nanotubes

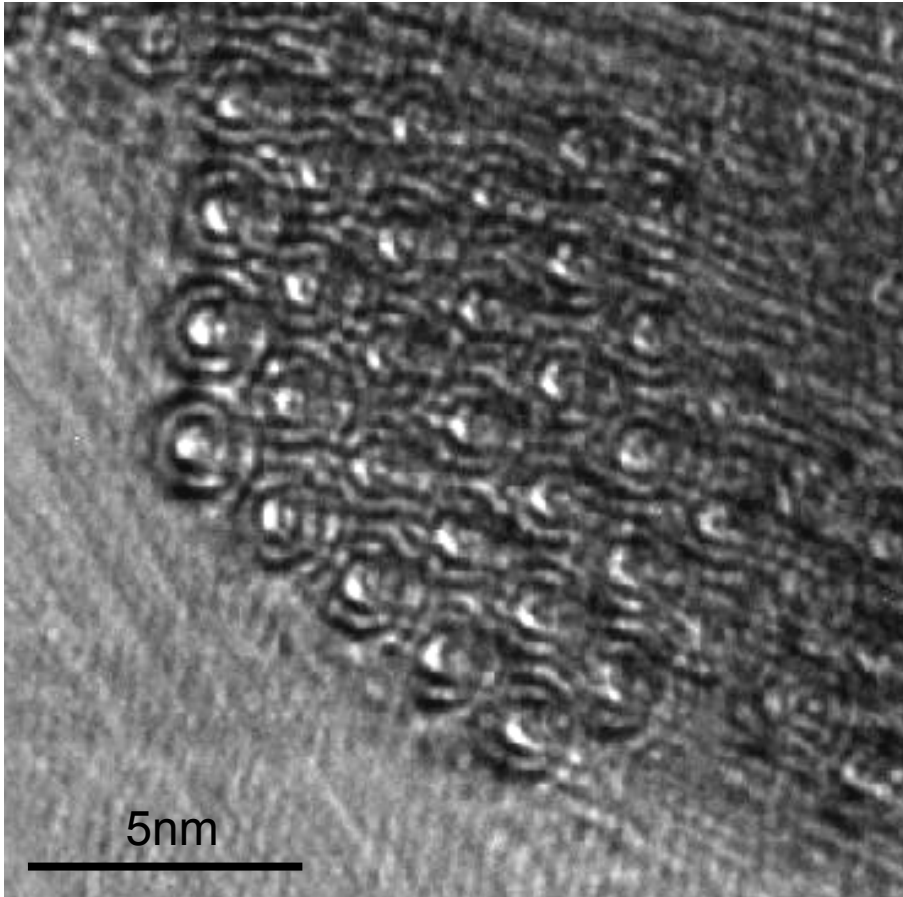


After purification : 90% of nanotubes

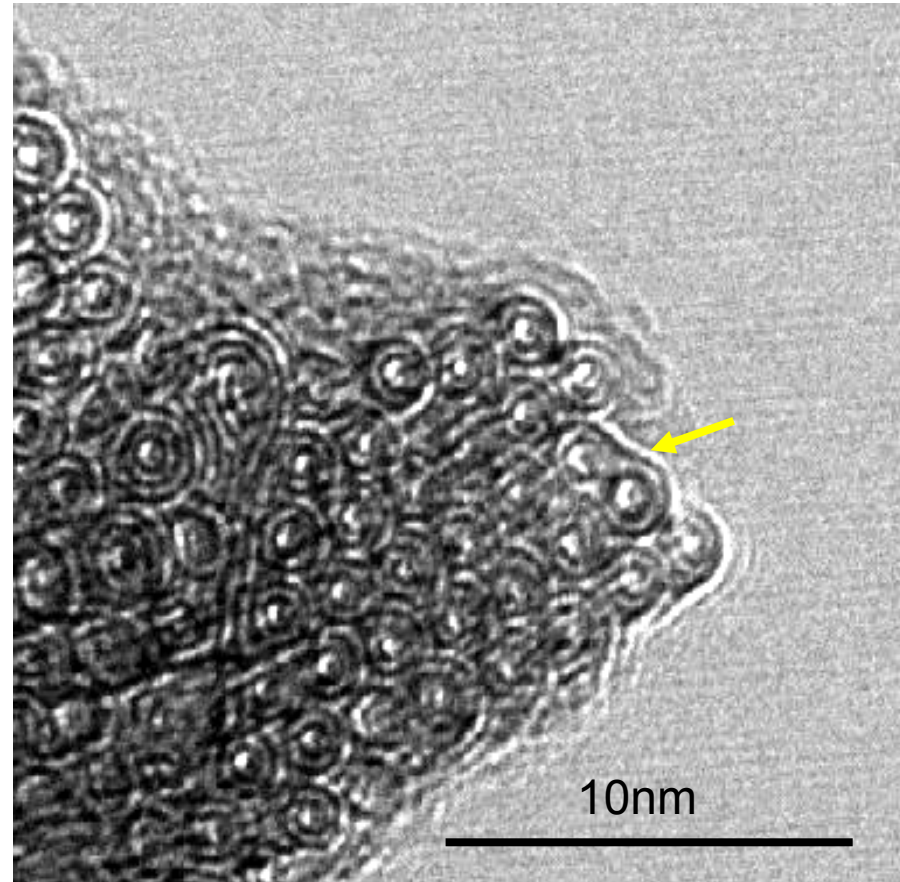


DWNT coalescence by heat treatment

High resolution TEM images of DWNTs doped with B (B.S. #6)



Heat treated at 1200°C

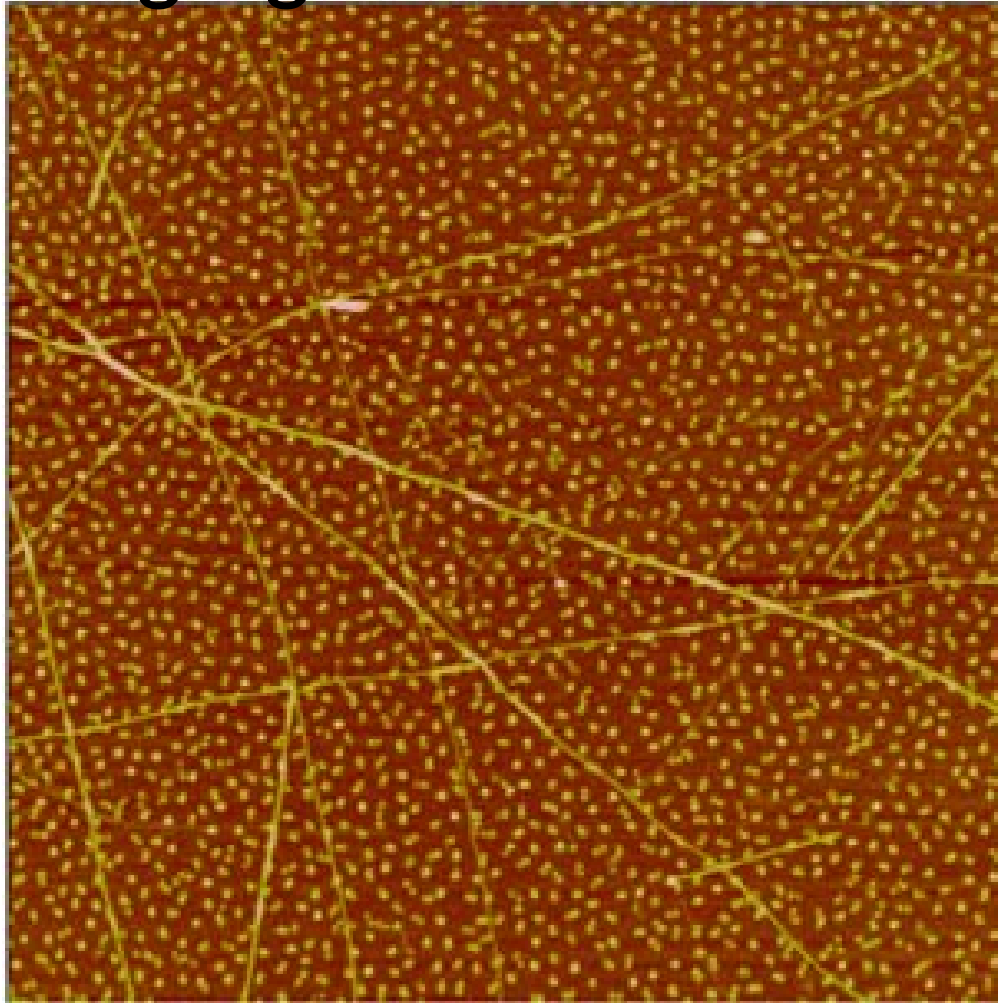


Heat treated at 1500°C

Coalescence of DWNTs outer shells are observed for 1500°C heat treatment

TEM images from M. Endo et al, Nano. Lett. (2005)

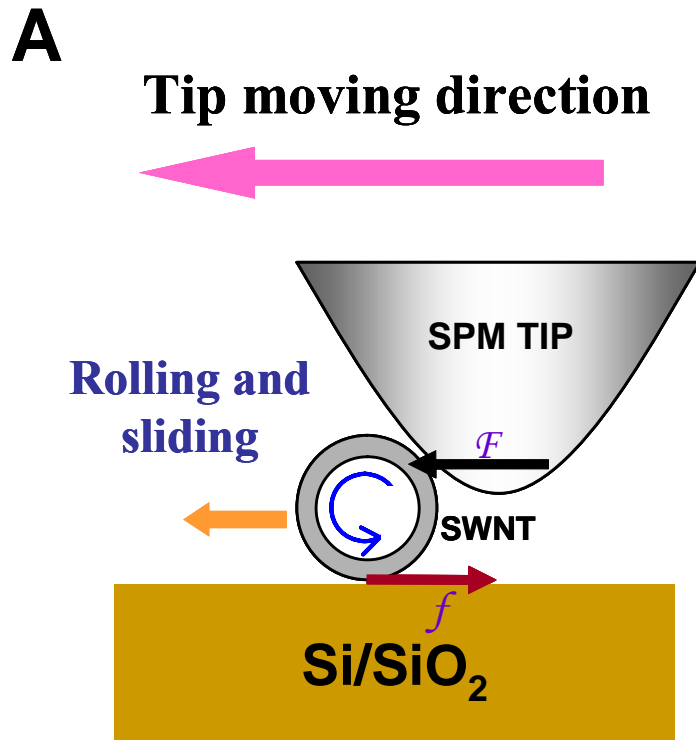
Imaging of SWNT Growth



AFM image of SWNTs grown by Co nanoparticles with ethanol CVD. The area is 2.5 X2.5um.

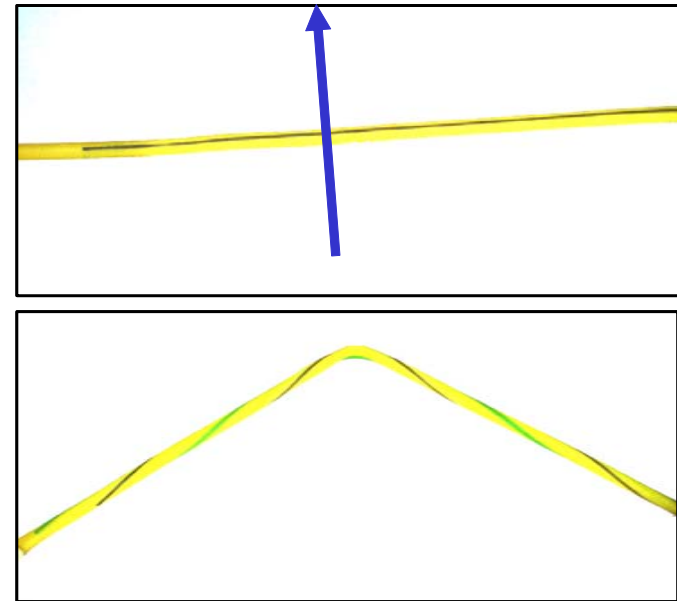
From J. Kong (unpublished)

SPM Tip produces rolling, sliding Motion



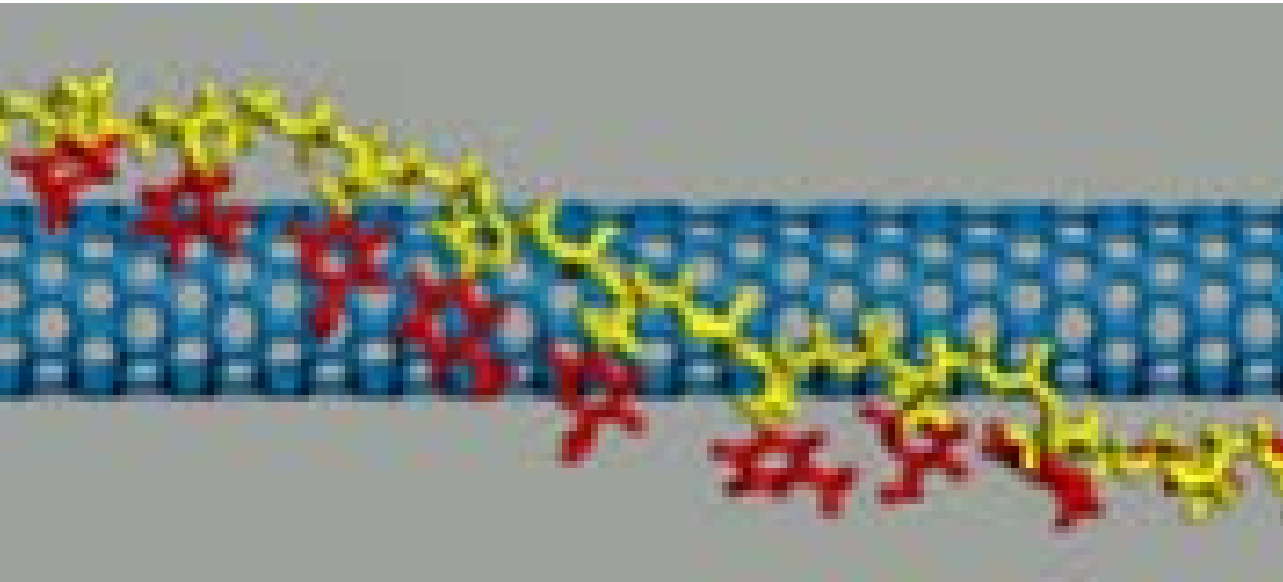
B

Macroscopic rubber tube model



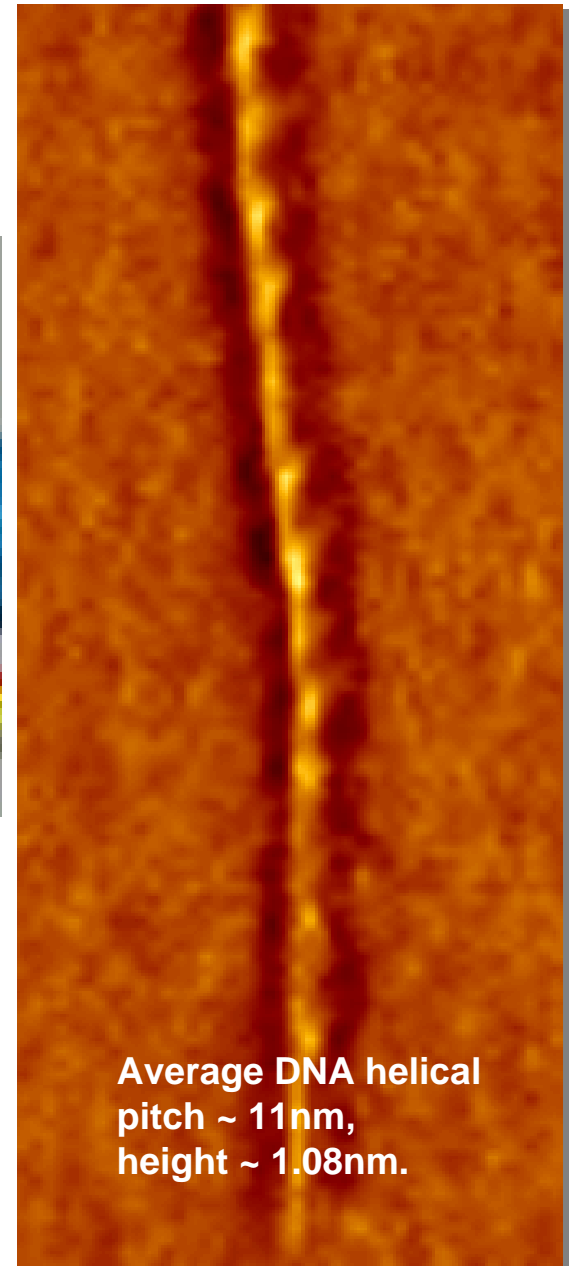
Effect of rolling and sliding motion of SWNT produced by scanning probe microscopy tip can be monitored by techniques such as Raman scattering

AFM for Imaging



Use of AFM to image a SWNT wrapped by DNA

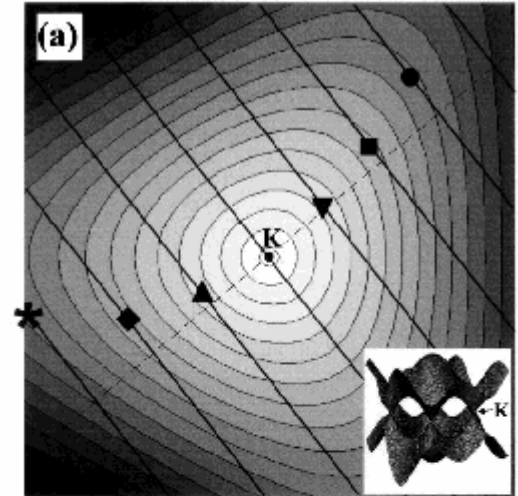
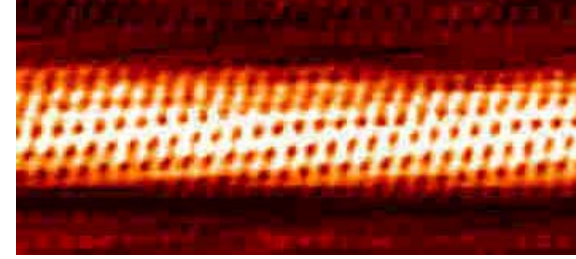
M. Zheng, *et al. Science* 302, 1546 (2003)



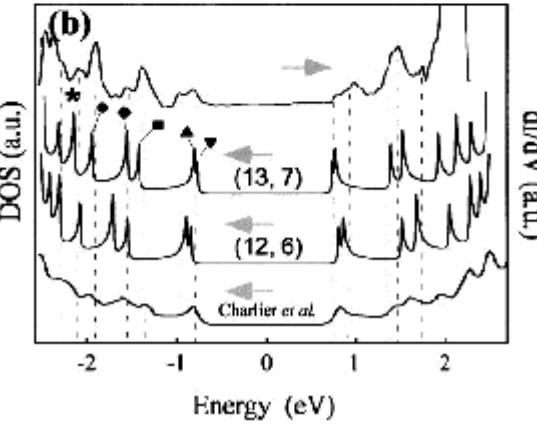
Average DNA helical
pitch ~ 11nm,
height ~ 1.08nm.

STM/STS

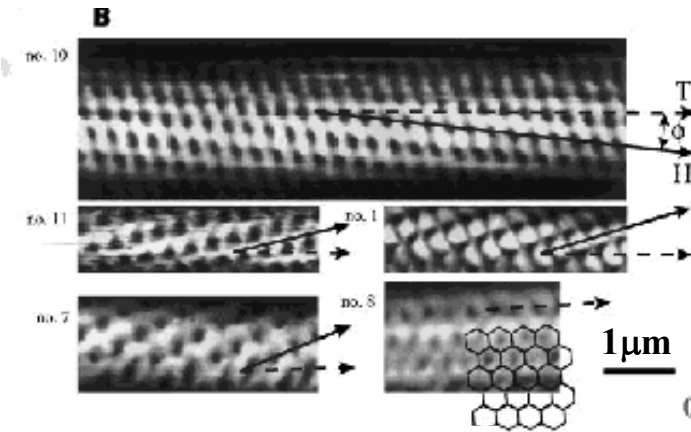
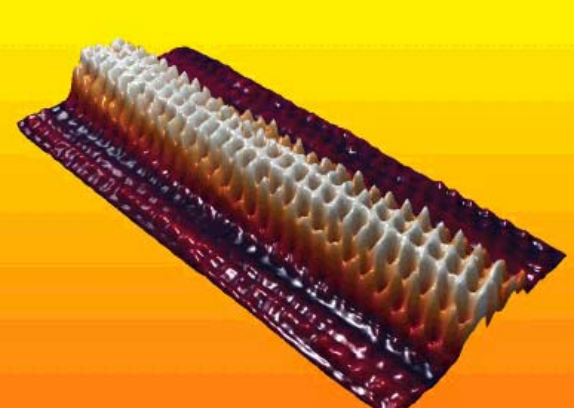
Geometric structure (STM)
and electronic density of states (STS)



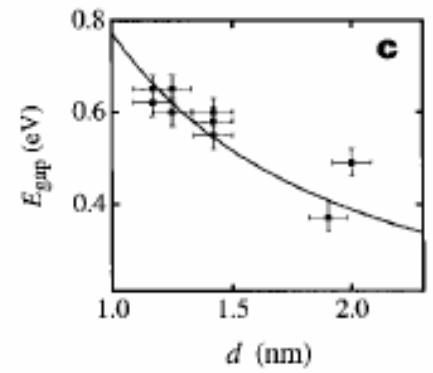
Cutting lines



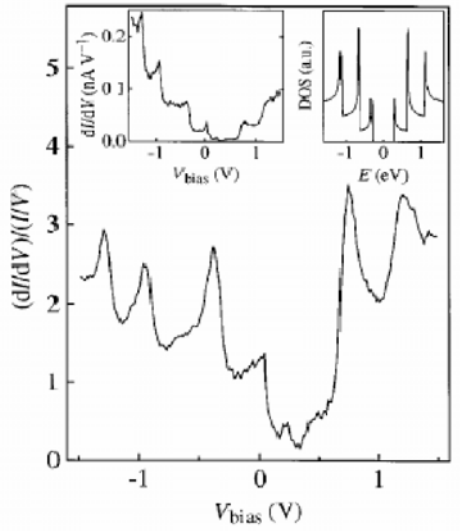
(13,7) nanotube



P. Kim et al.,
Phys. Rev. Lett.
82, 1225 (1999)

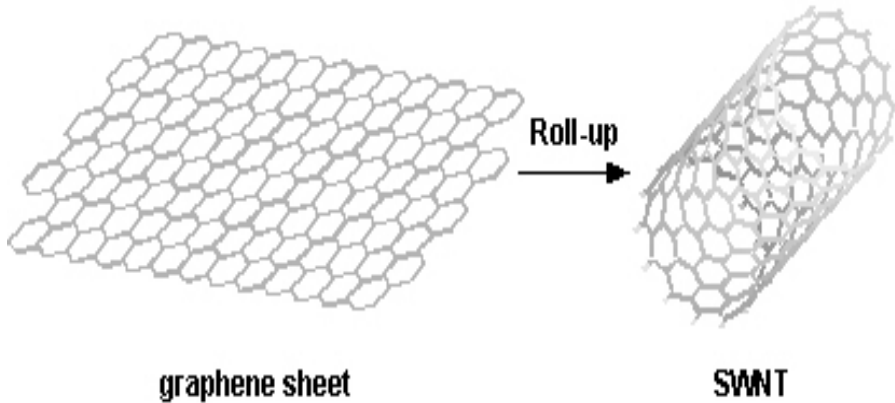


J. W. G. Wildoer et al.,
Nature 391, 59 (1998)

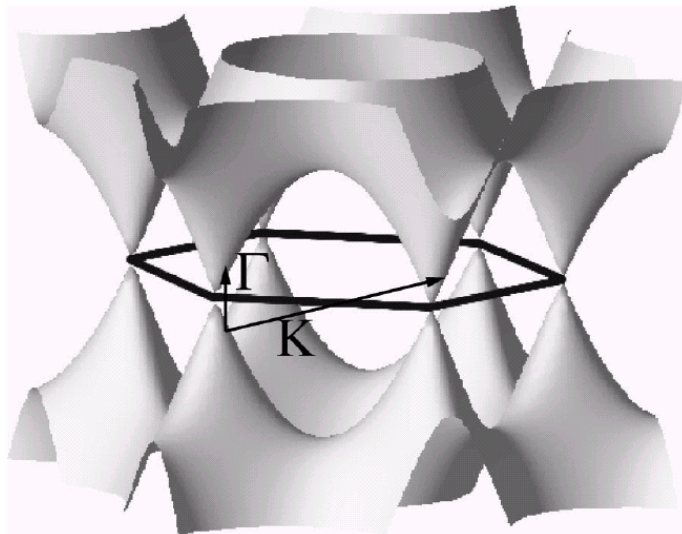
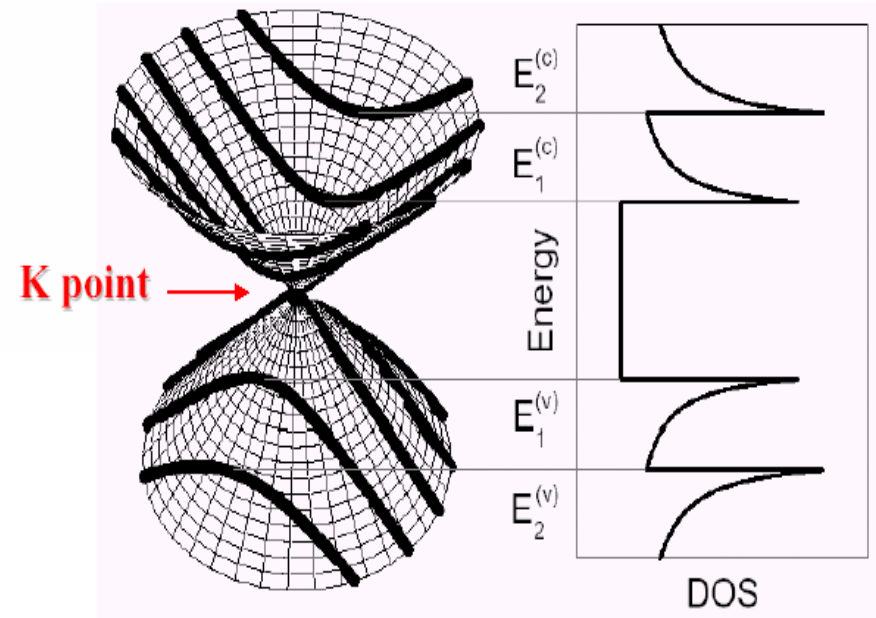


Electronic structure of a carbon nanotube

Rolling up 2D graphene sheet



Confinement of 1D electronic states



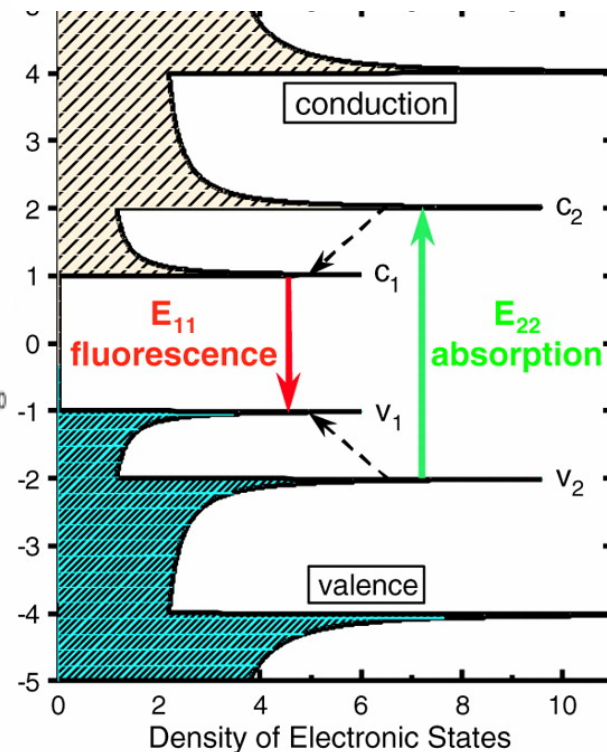
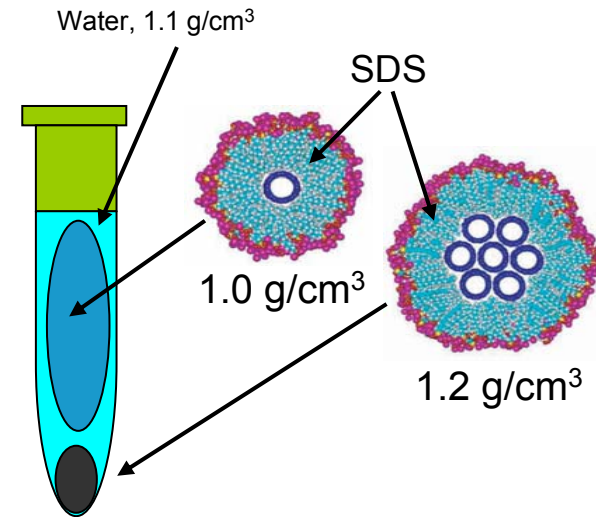
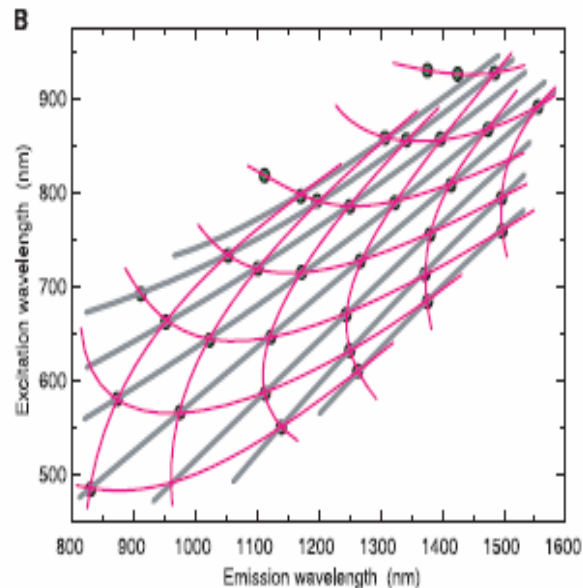
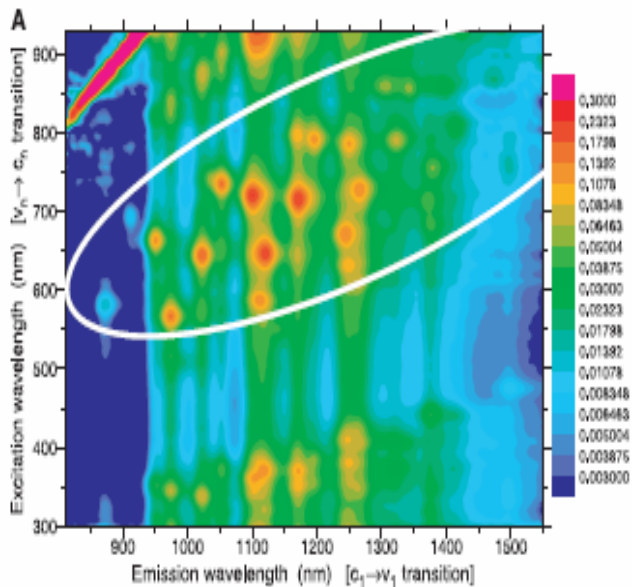
1D van Hove singularities - high density of electronic states (DOS) at well defined energies

Outline on Characterization with a Focus on optical characterization

- **What is in my sample?**
- **What we can learn from:**
 - **Photoluminescence?**
 - **Raman spectroscopy?**
 - **Fast Optics?**

Photoluminescence Measurements

- Nanotubes dispersed in aqueous solution using surfactants
- Only semiconducting tubes are seen



- Identified Ratio problem and family effect

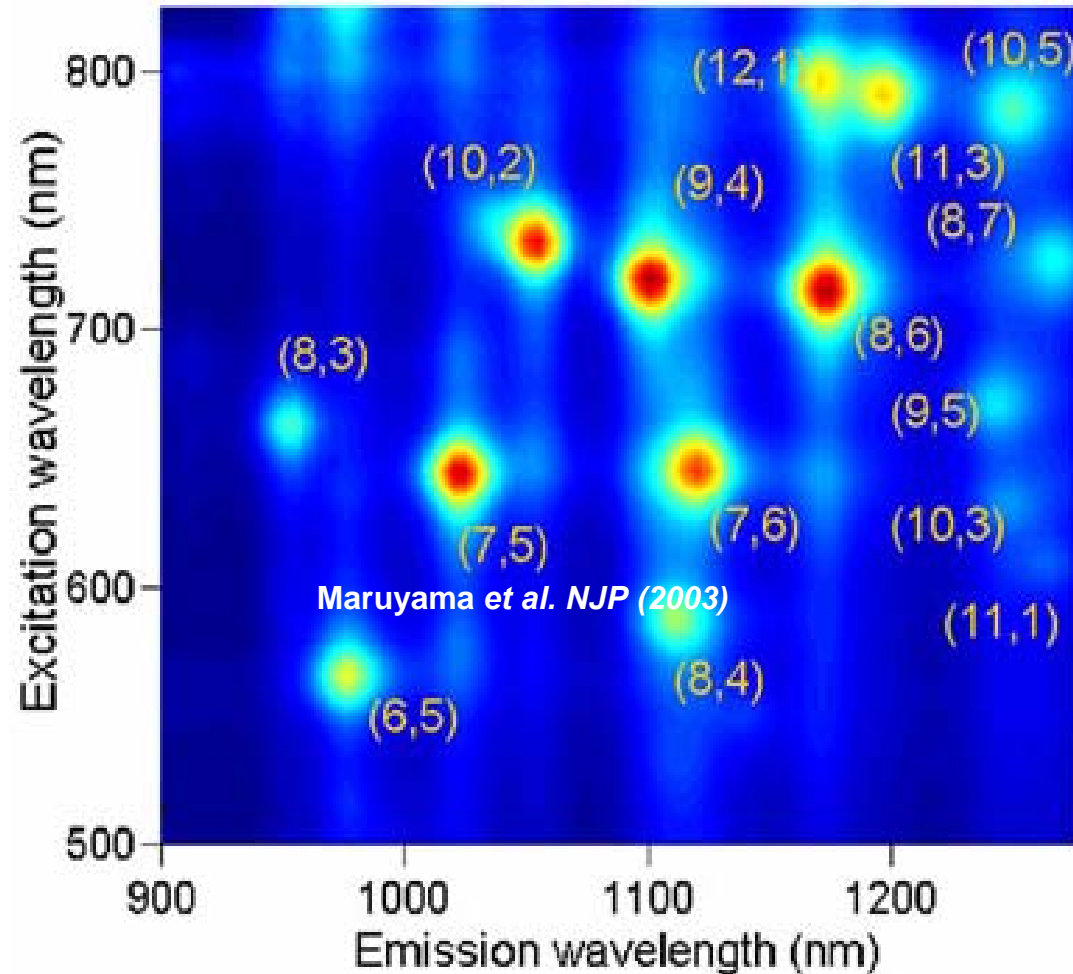
- O'Connell et al., Science 297, 593 (2002)
- Bachilo et al., Science 298, 2361 (2002)

Nanotube PL Spectroscopy

Most Measurements

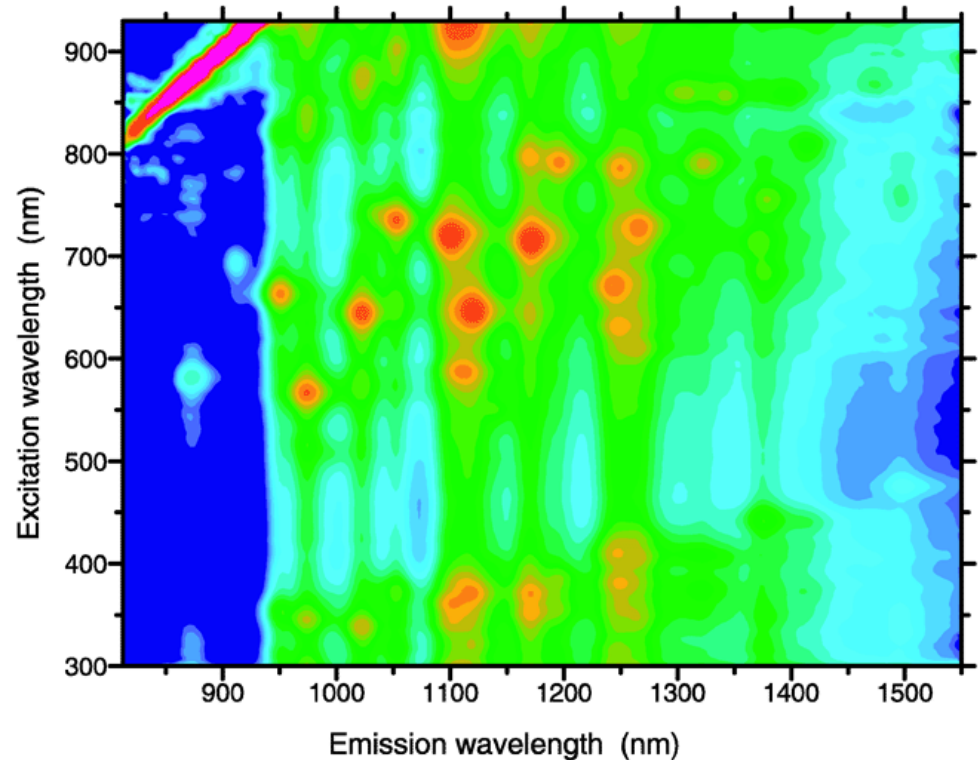
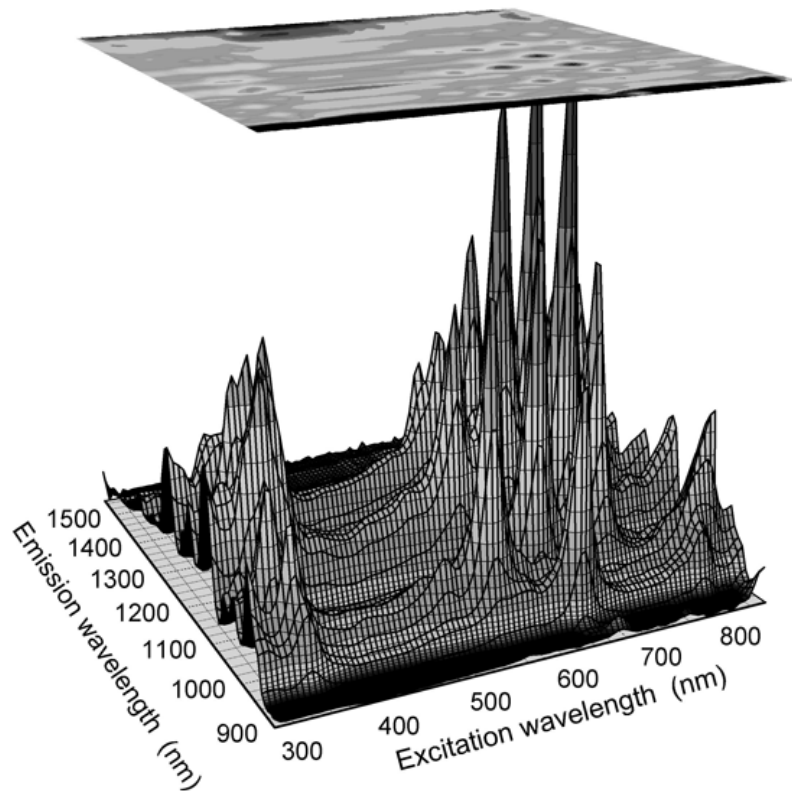
- excitation at E_{22} , emission at E_{11}
- measured with Xe lamp
- Solution allows PL measurements on many SWNTs at once
- Allows excitation vs emission maps to be made
- $(2n+m)$ family patterns give (n, m) identifications.

PL map of SDS- dispersed HiPco CNTs



PHOTOLUMINESCENCE

Data are shown as 2D and 3D maps



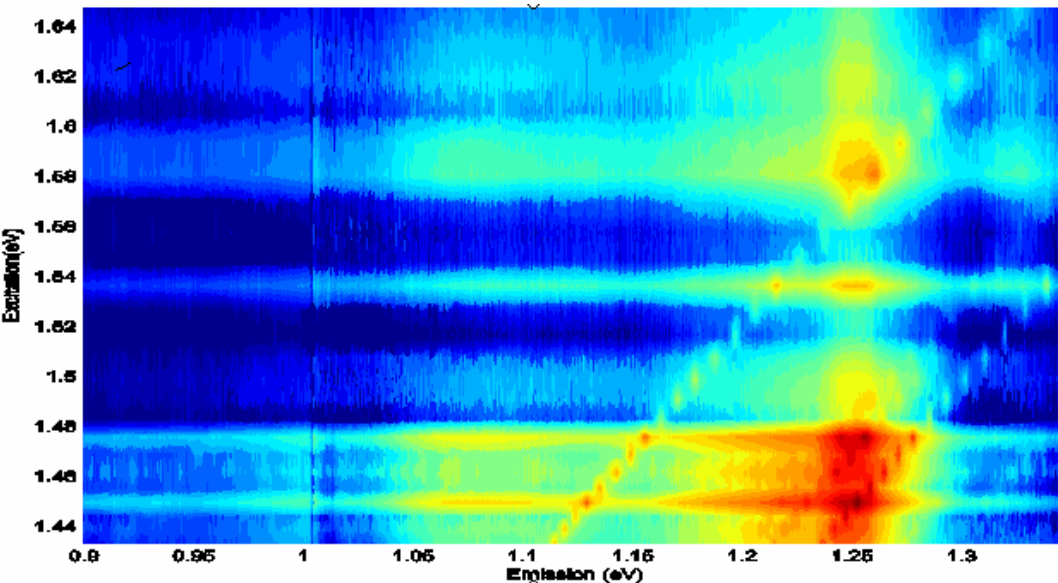
The observation of intensity and energy maps strongly influenced other photophysics characterization techniques for carbon nanotubes

S. M. Bachilo et al., Science 298, 2361 (2002)

Laser photoluminescence excitation spectroscopy (PLE)



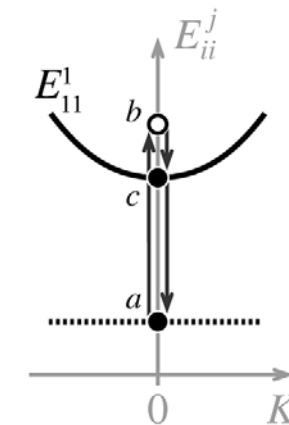
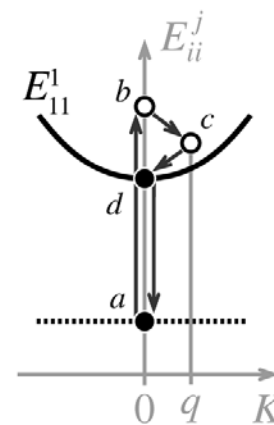
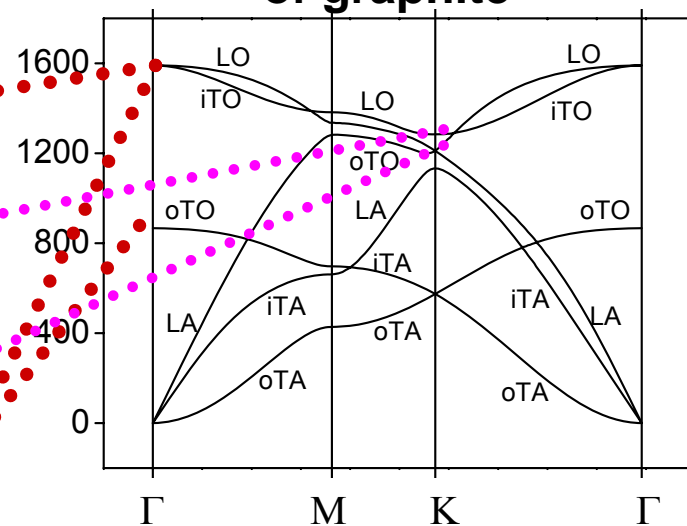
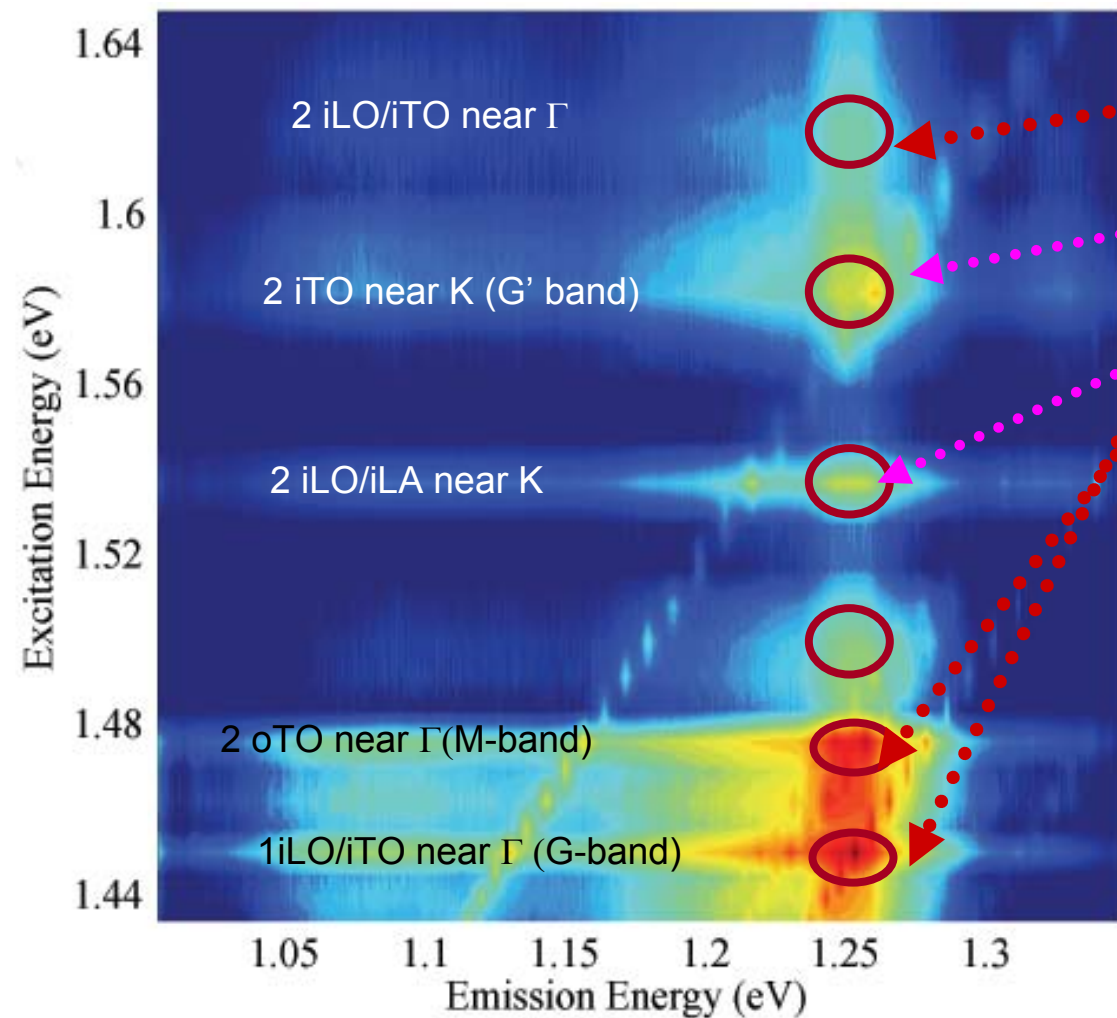
- Can be done with laser excitations
- Ar⁺ pumped Ti:Sapphire laser.
- Ar⁺ pumped Dye laser
- Spex 750M monochromator.
- Low temp (350 – 1.5K).
- InGaAs diode array.
- LN₂ cooled CCD camera.



-For a special sample with a large concentration of (6,5) SWNTs allows study of phonon-assisted excitation and emission for specific phonons

Emission Identified with One and Two Phonon Processes:

Phonon dispersion relations of graphite

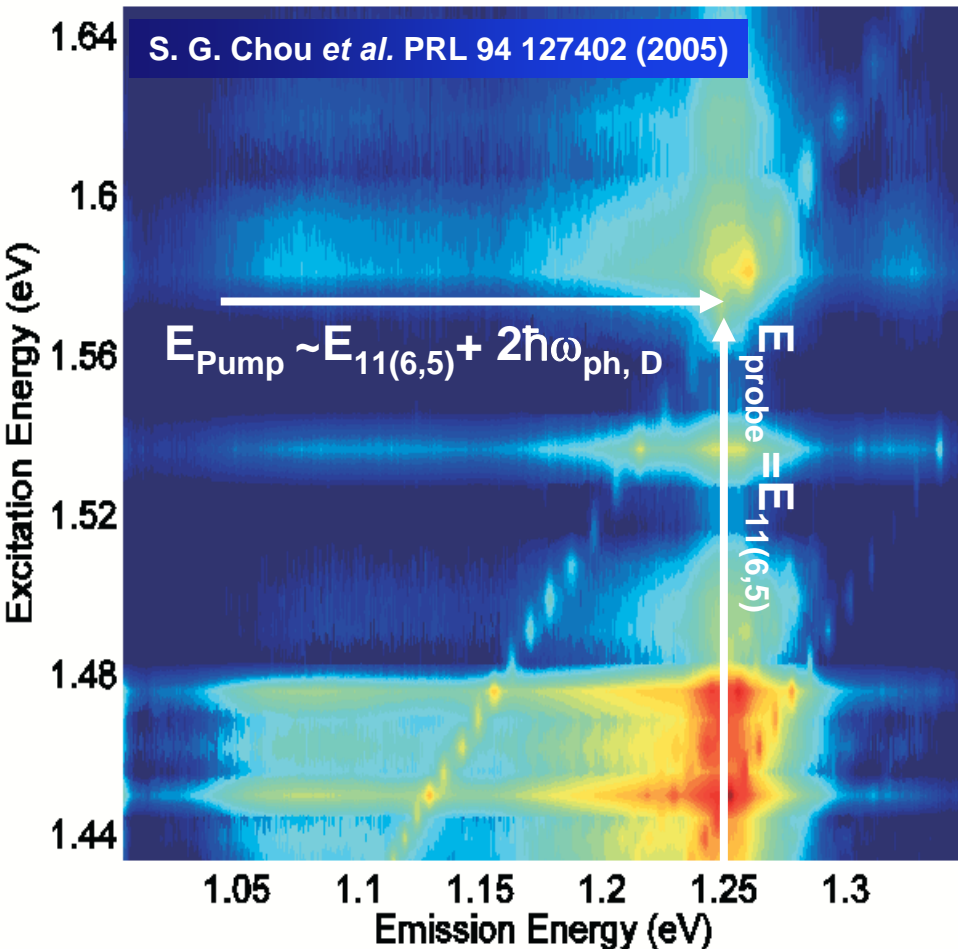


Two phonon process

One phonon process

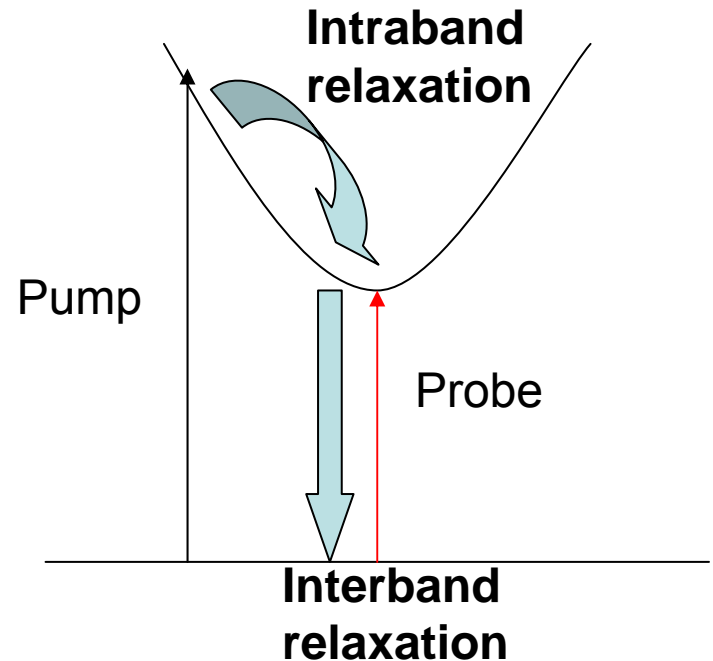
Non-degenerate Pump-Probe

Frequency domain



Fast optics, Time domain

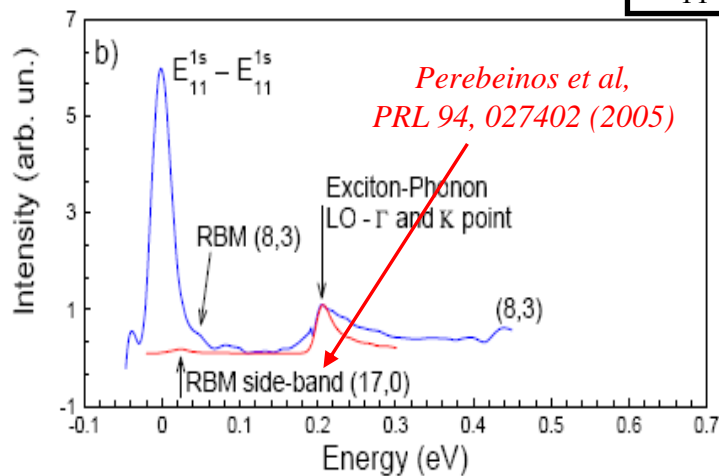
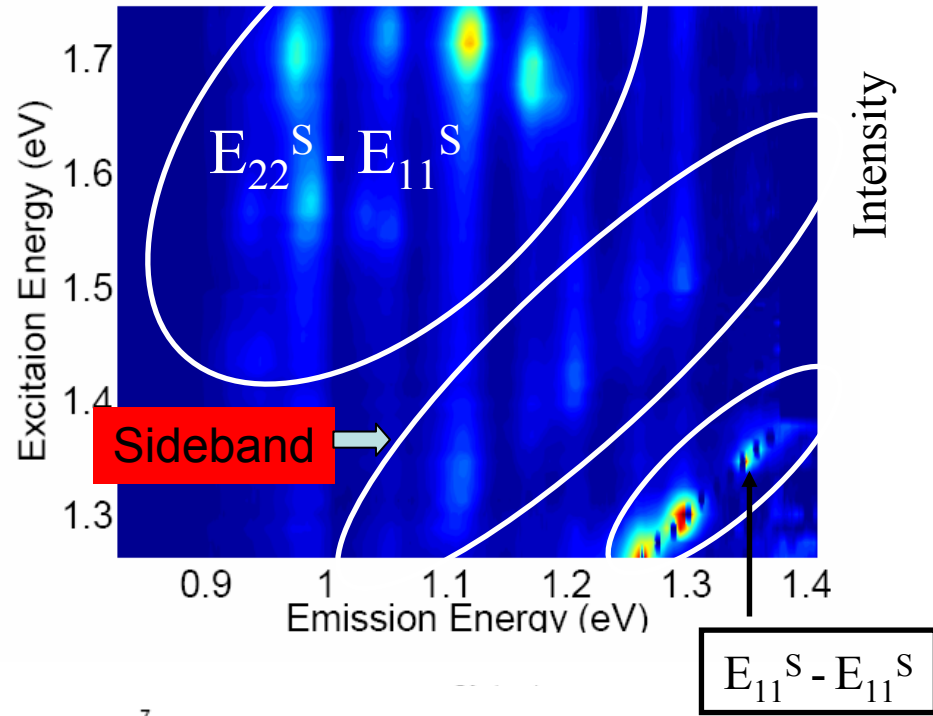
$E_{\text{pump}} = 1.57 \pm 0.01 \text{ eV}, \sim E_{11}(6,5) + 2\hbar\omega_{\text{D}}$
 $E_{\text{probe}} = \text{around } E_{11} \text{ of } (6,5) \text{ nanotube}$
(Instrument resolution $\sim 250\text{fs}$)



S. G. Chou *et al.* PRB 72 195415 (2005)

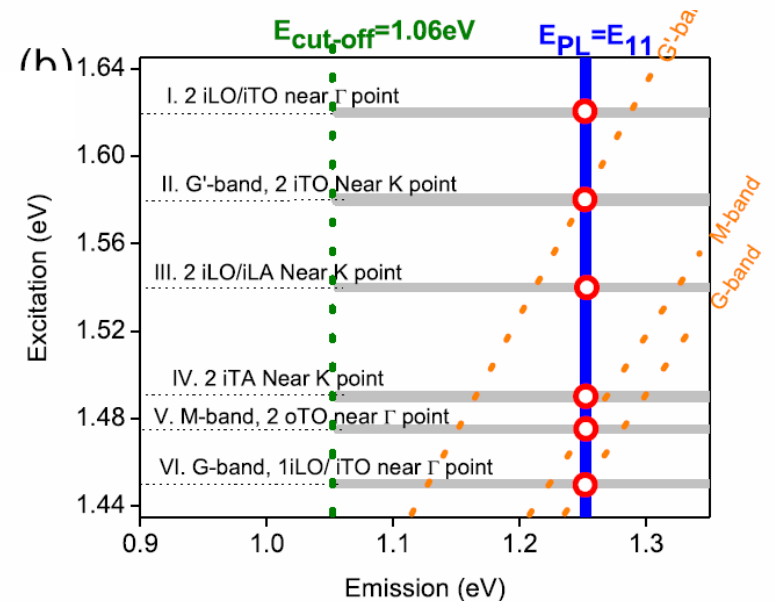
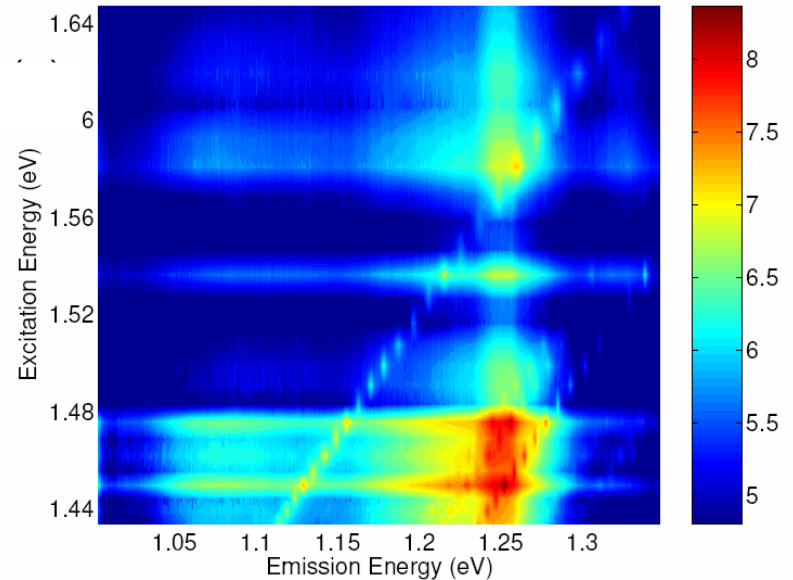
Exciton-phonon sidebands and Phonon-Assisted Processes

HiPco + SDS solution



Plentz et al. PRL 95, 247401 (2005)

CoMoCAT+DNA – (6,5) enriched

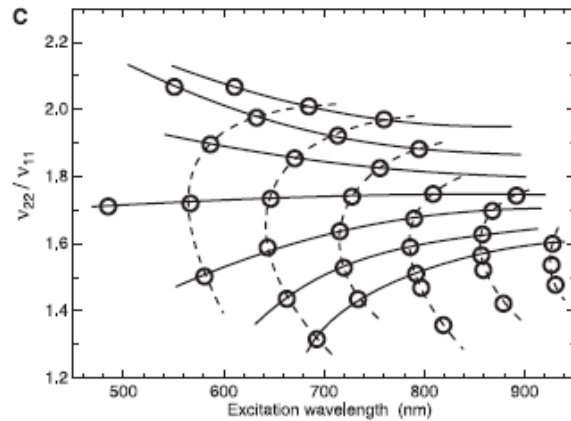
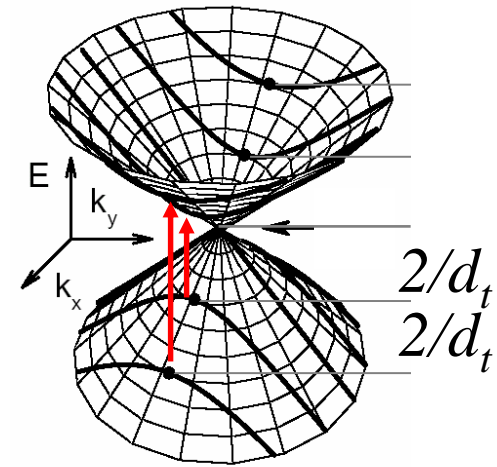
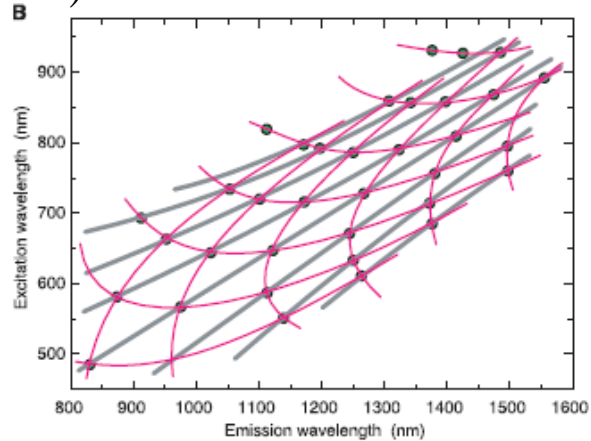
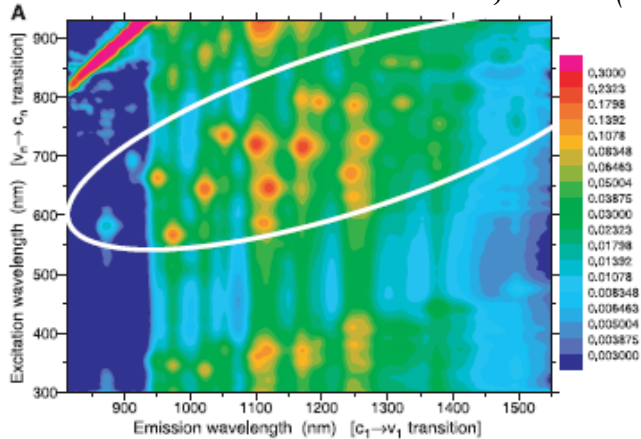


Chou et al. PRL 94, 127402 (2005)

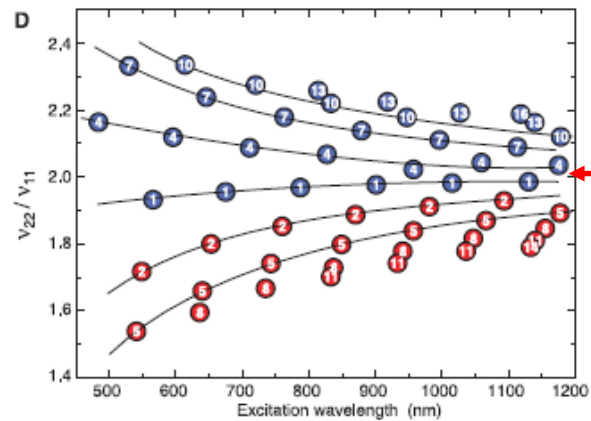
The ratio problem for E_{22}^S and E_{11}^S

E_{22}^S / E_{11}^S equals 1.75 instead of 2!

Bachilo et al. Science 298, 2361(2002)



-STB

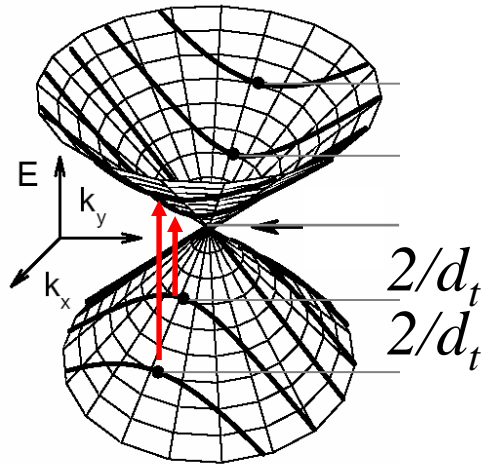


-ETB

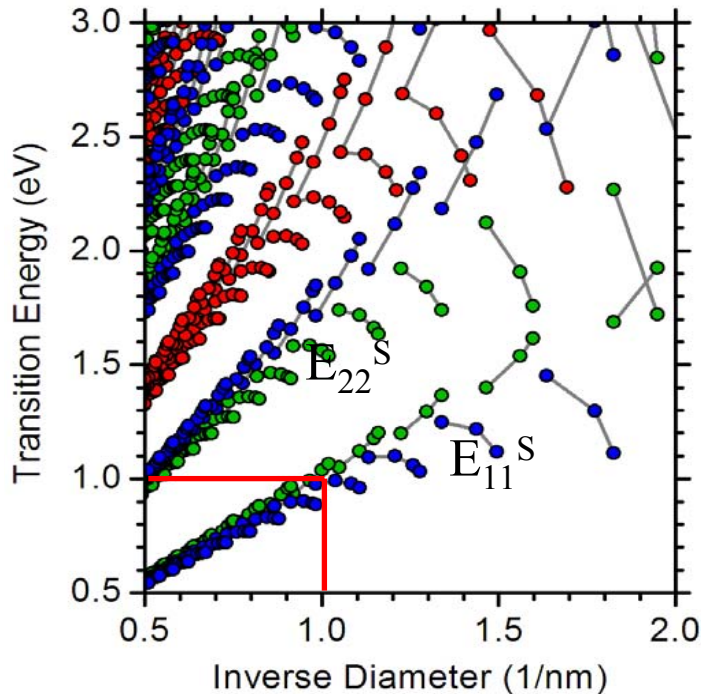
For a linear dispersion
 $E_{22}^S / E_{11}^S = 2$

- This work established family behavior and led to consideration of many body effects

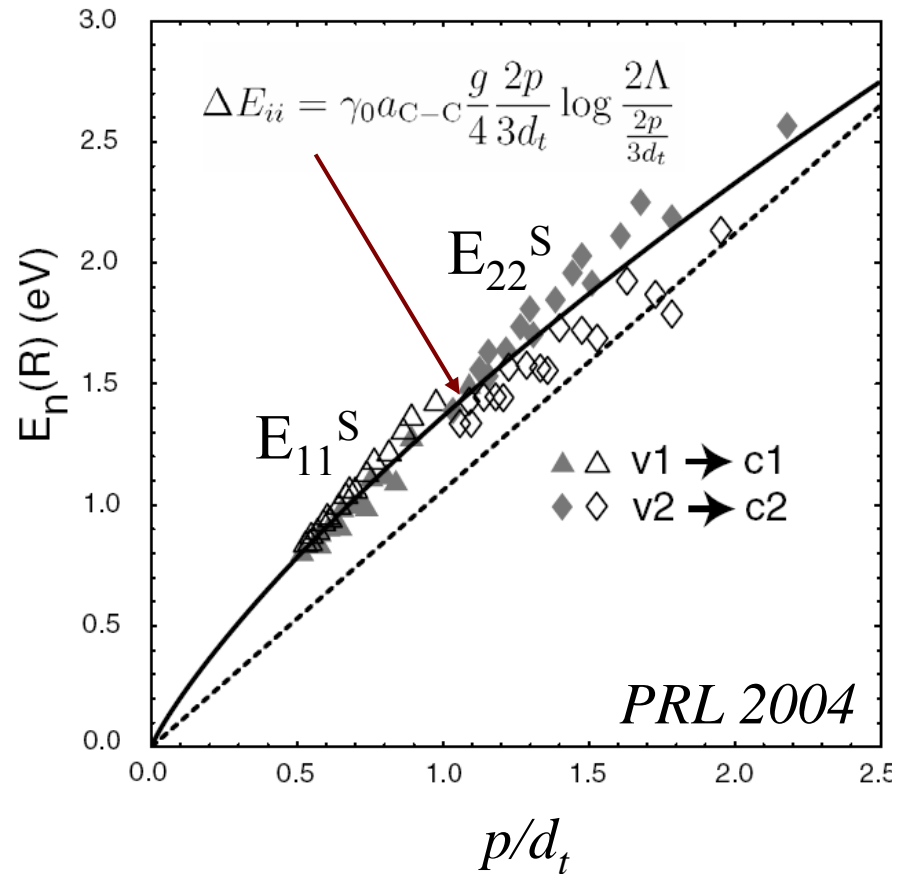
The big picture: E_{ii} obeys a scaling law



$$E_{11}(d_t) = E_{22}(d_t/2)$$



E_{11}^S and E_{22}^S follow a single scaling law when plotted as a function of p/d_t



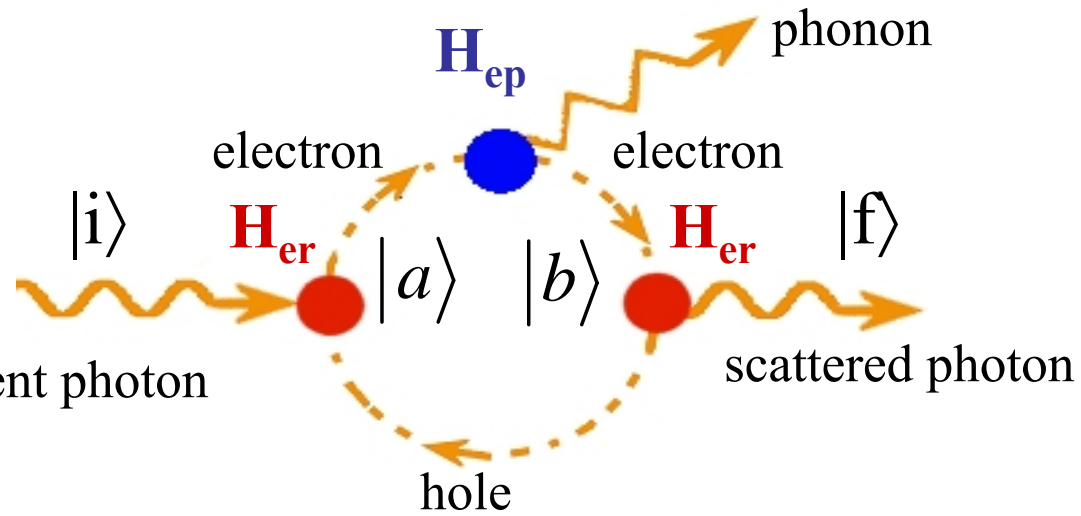
$$p = \Gamma^I \Gamma^S \Gamma^3 \Gamma^4 \dots \Gamma^{\text{tot}} E_2^{\text{II}}, E_2^{\text{SS}}, E_W^{\text{II}}, E_2^{\text{33}}, E_2^{\text{IV}} \dots$$

Kane & Mele, PRL 90, 207401 (2003)

Outline on Characterization with a Focus on optical characterization

- **What is in my sample?**
- **What we can learn from:**
 - **Photoluminescence?**
 - **Raman spectroscopy?**
 - **Fast Optics?**

Resonant Raman scattering process



$$|n_i, n_s; n_q; \psi_e\rangle$$

photons (green arrow pointing to n_i, n_s)
 phonon (red arrow pointing to n_q)
 electron (blue arrow pointing to ψ_e)

- Stokes process – phonon creation
- Anti-Stokes – phonon annihilation

Raman intensity \rightarrow transition probability per unit time

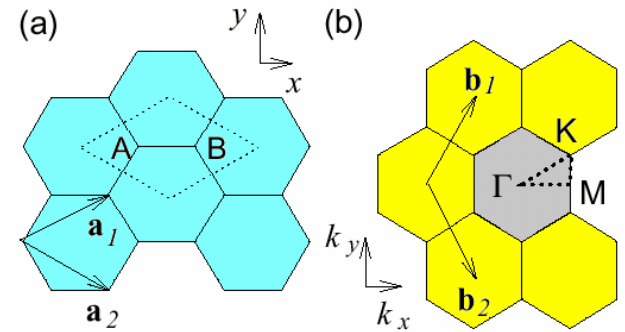
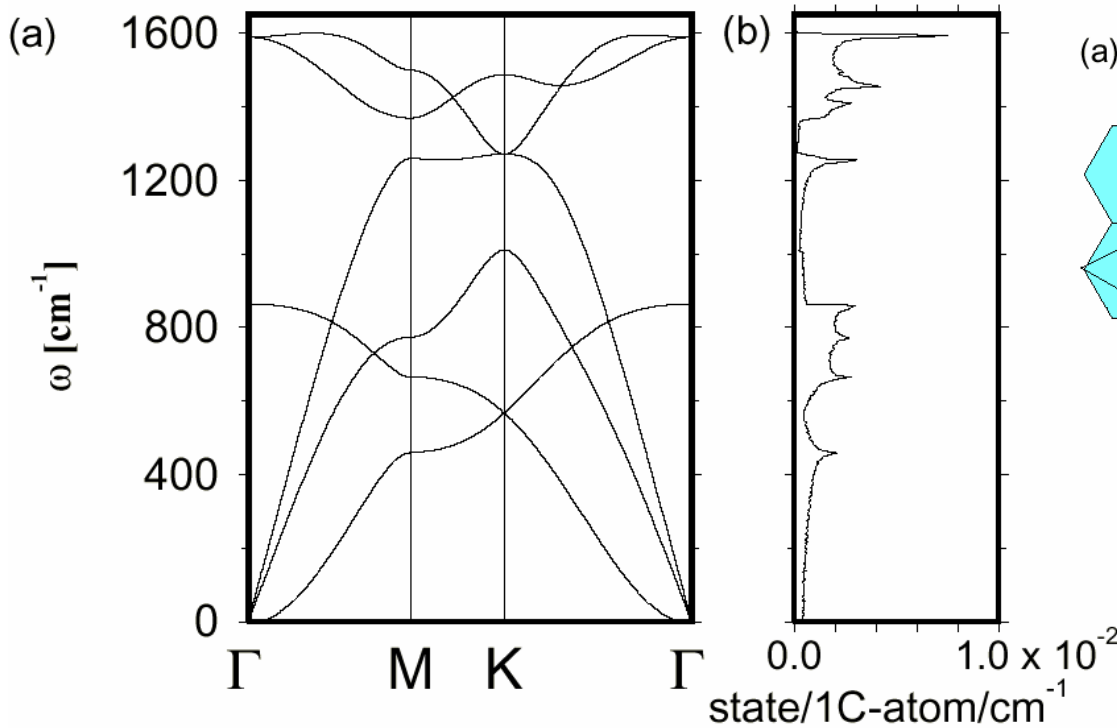
$$I(E_i) = C \left| \sum_{a,b} \frac{\langle f | H_{e-r} | b \rangle \langle b | H_{e-ph} | a \rangle \langle a | H_{e-r} | i \rangle}{(E_i - E_a - i\gamma)(E_i - E_b - i\gamma)} \right|^2$$

$$E_i - E_a = \hbar\omega_i - \Delta\varepsilon \quad \longrightarrow \quad \text{resonance with incident photon}$$

$$E_i - E_b = \hbar\omega_i \mp \hbar\omega_q - \Delta\varepsilon = \hbar\omega_s - \Delta\varepsilon \quad \longrightarrow \quad \text{resonance with scattered photon}$$

Phonon Dispersion of 2D graphite

- E_{2g2} Raman mode at 1580cm^{-1}

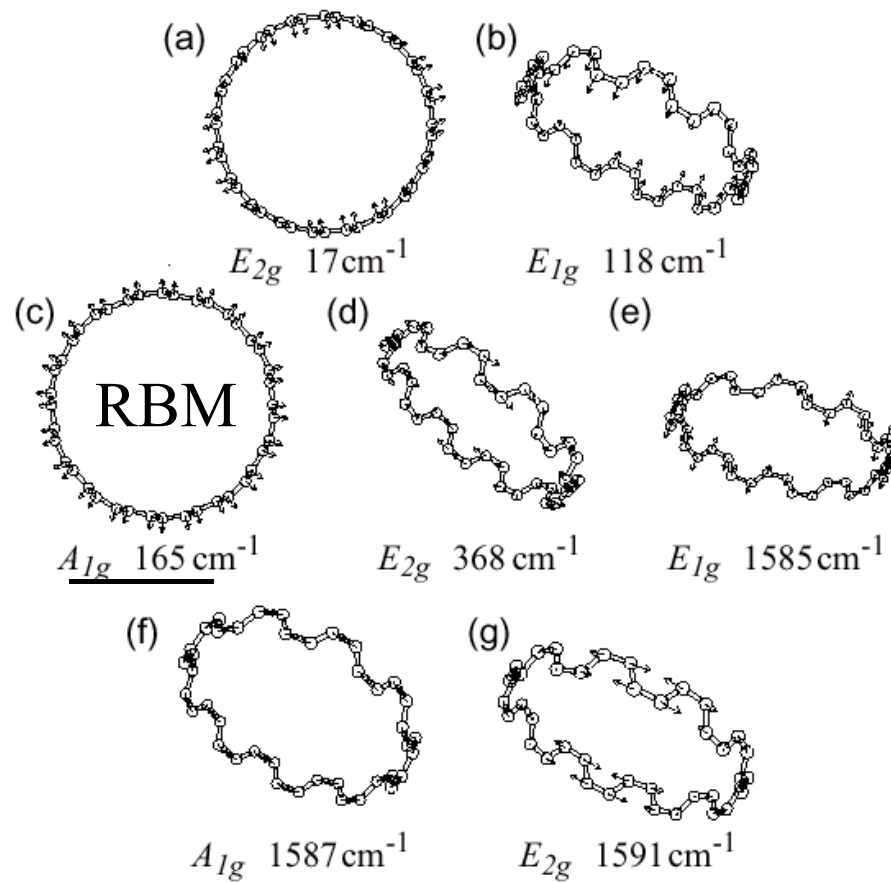
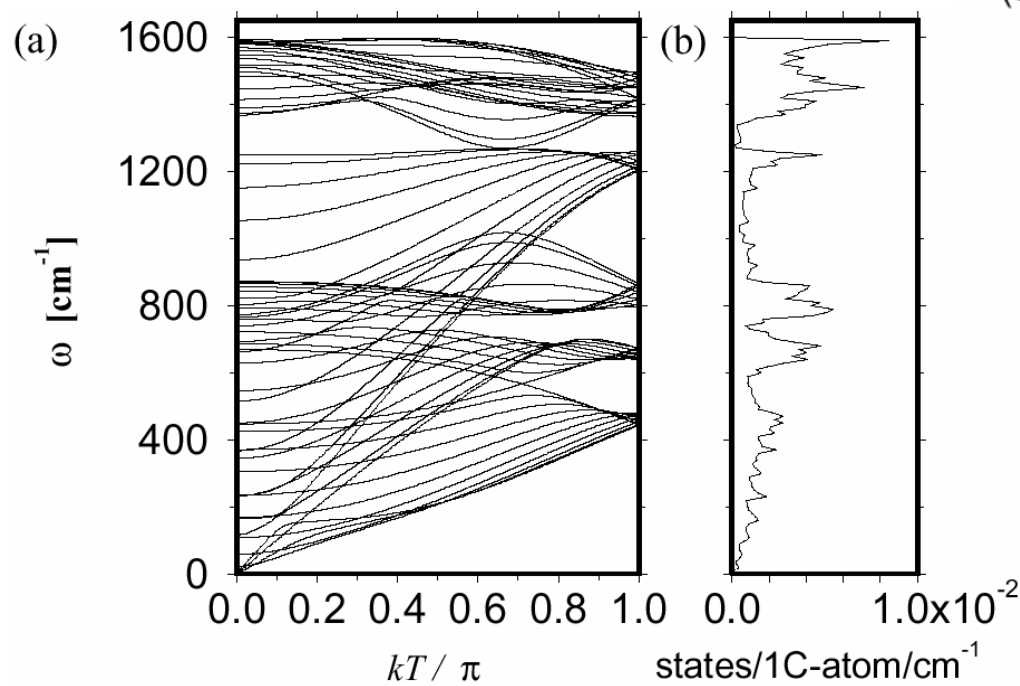


R. Saito, M.S. Dresselhaus
and G. Dresselhaus
“Physical Properties of
Carbon Nanotubes”
Imperial College Press
(1998)

Phonon modes -- (10,10) Armchair

R.Saito *et al. Phys. Rev.* **B57** (1998) 4145

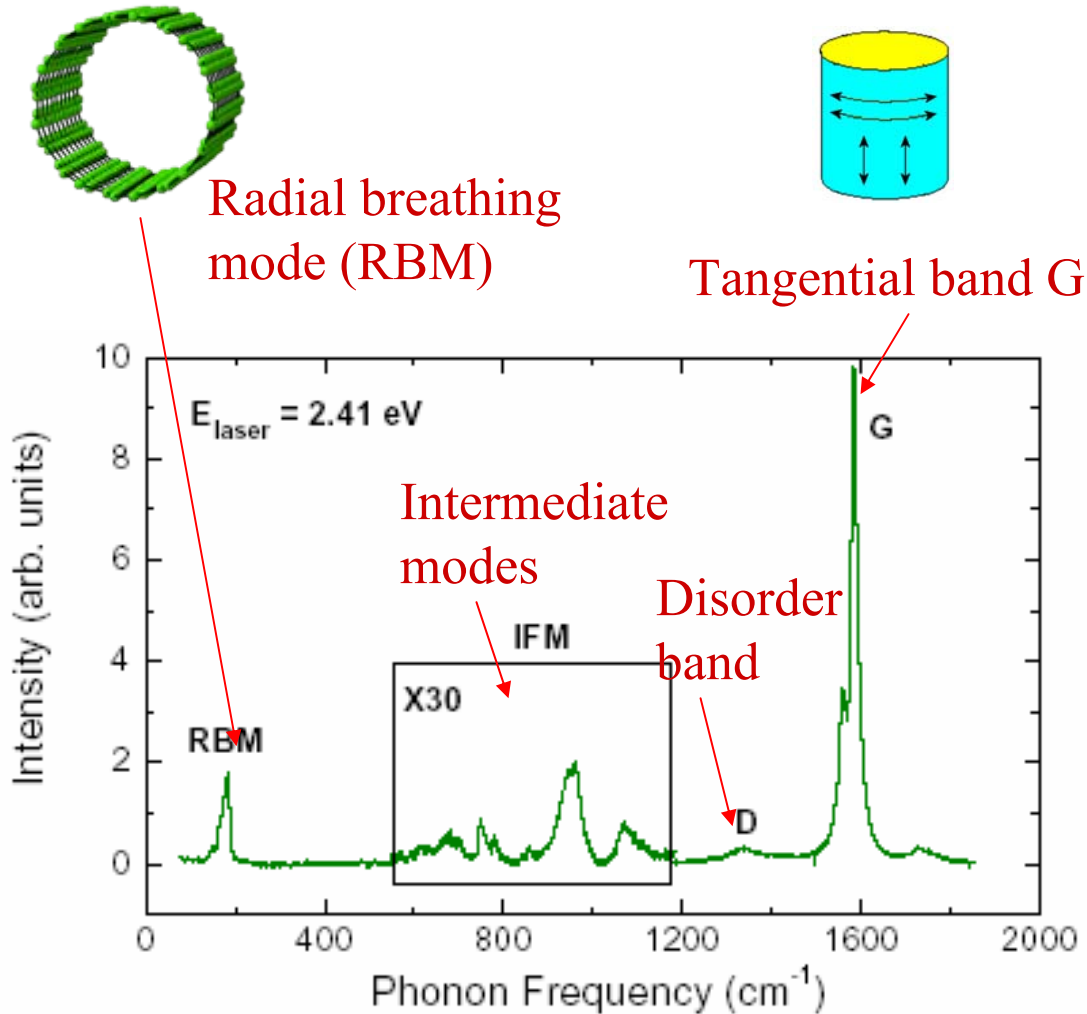
- $N=20$, $6N=120$ phonon modes
- 66 distinct, 4 acoustic
- 16 Raman (Group theory)
- A_1 , A_2 , E_1 symmetry modes are Raman active



7 Raman intensive modes

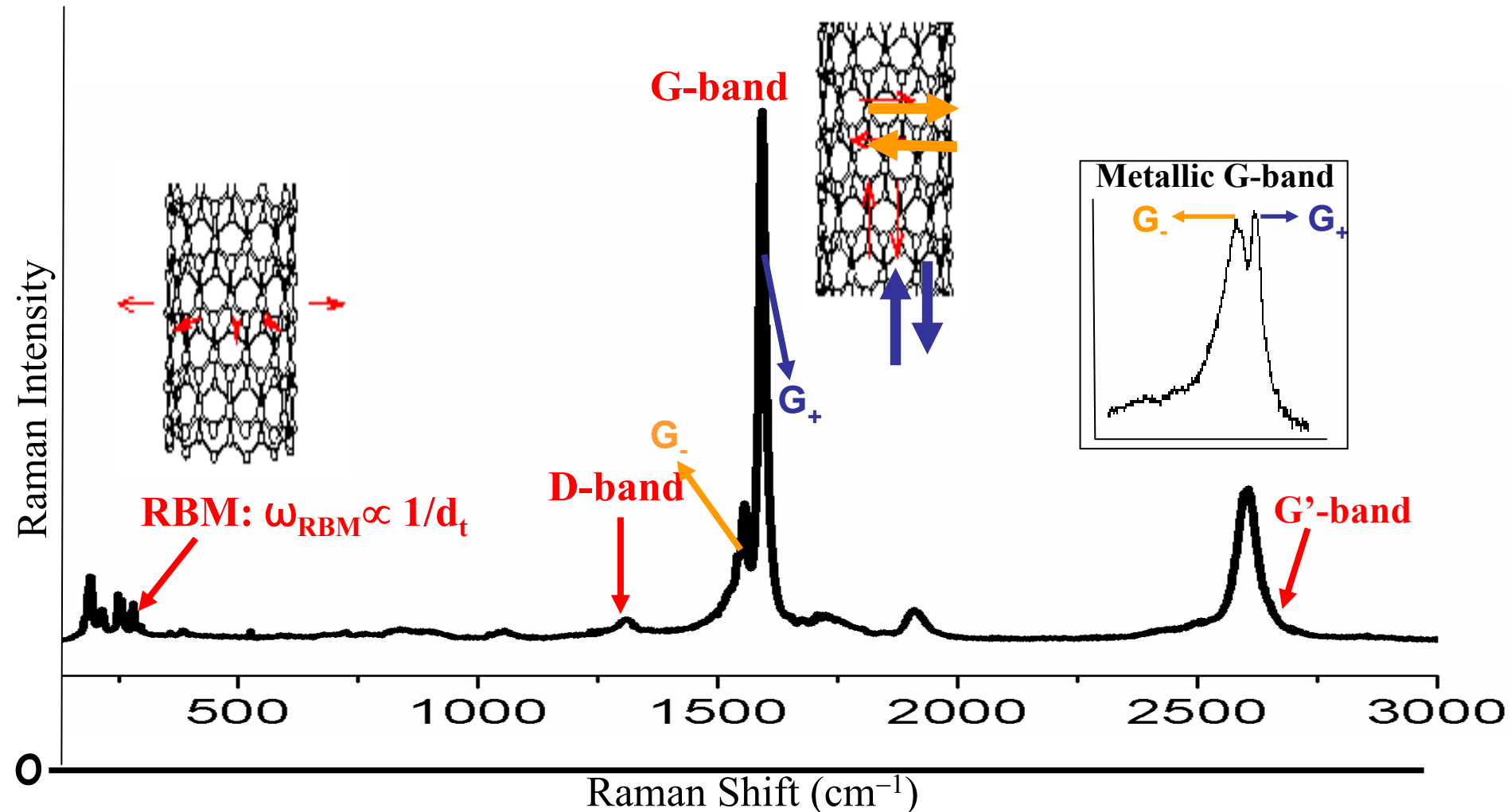
Raman spectra of carbon nanotubes

First-order spectral range



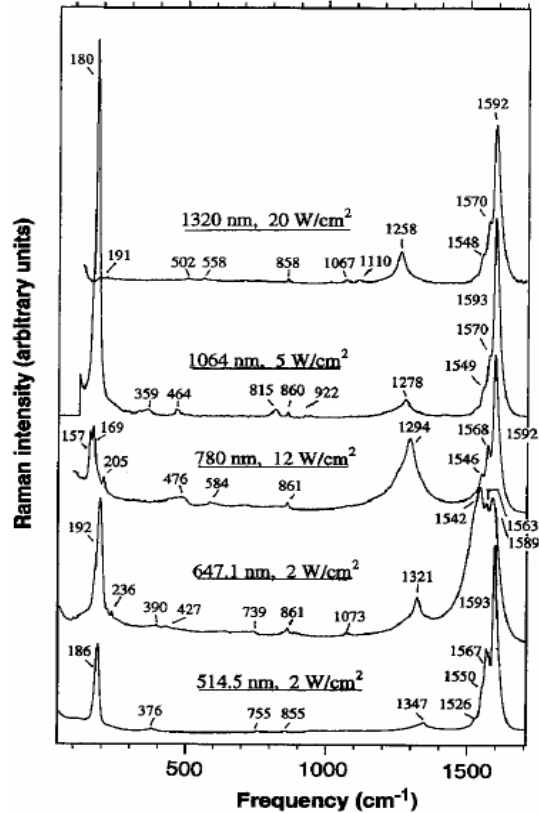
The presence of the RBM and the special G-band doublet gives signature of small diameter (< 2 nm)) carbon nanotubes in your sample

Raman Spectra of SWNT Bundles

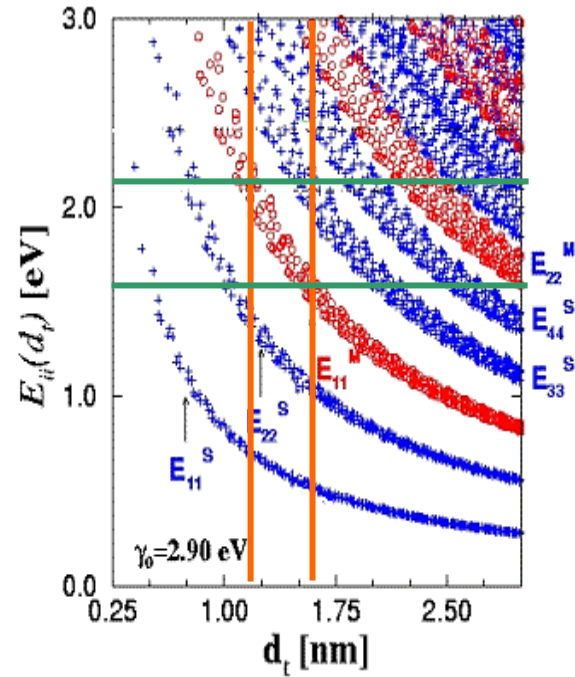
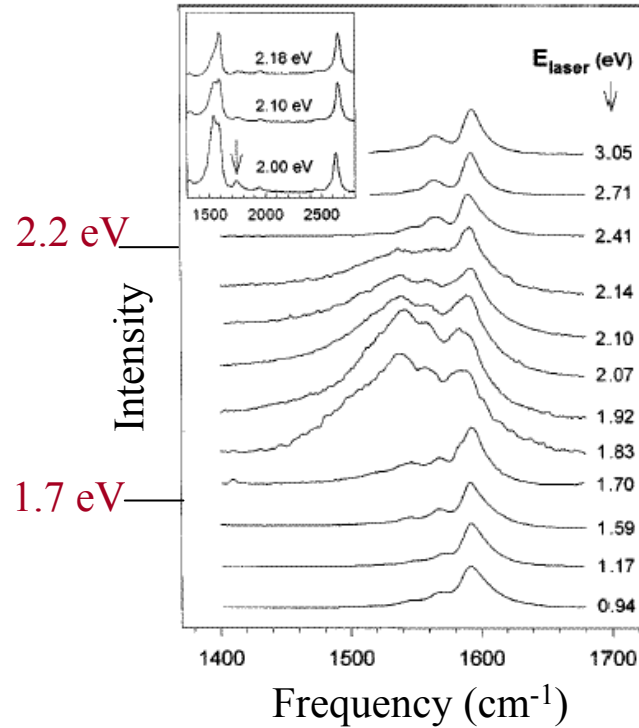


- RBM gives tube diameter and diameter distribution
- Raman D-band characterizes structural disorder
- G₋ band distinguished M, S tubes and G₊ relates to charge transfer
- G['] band (2nd order of D-band) provides connection of phonon to its wave vector

Resonant Raman scattering in carbon nanotubes



A. M. Rao *et al.*, *Science*
275 (1997) 187



M. A. Pimenta *et al.*
Phys. Rev. B, **58**,
 R16016, (1998)

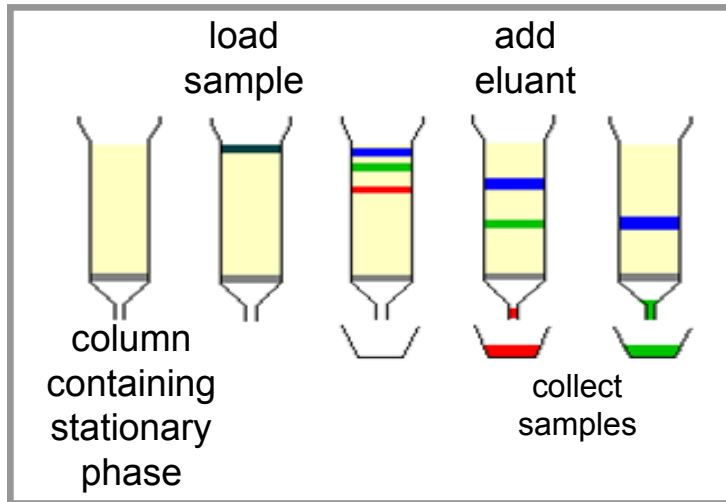
- Resonance Raman process
- Raman lineshape can distinguish metallic and semiconducting nanotubes
- Kataura plots relate the E_{ii} to (n,m) tubes



DNA-Assisted SEPARATION



M. Zheng *et al.*, *Science*, **302**, 1546 (2003).



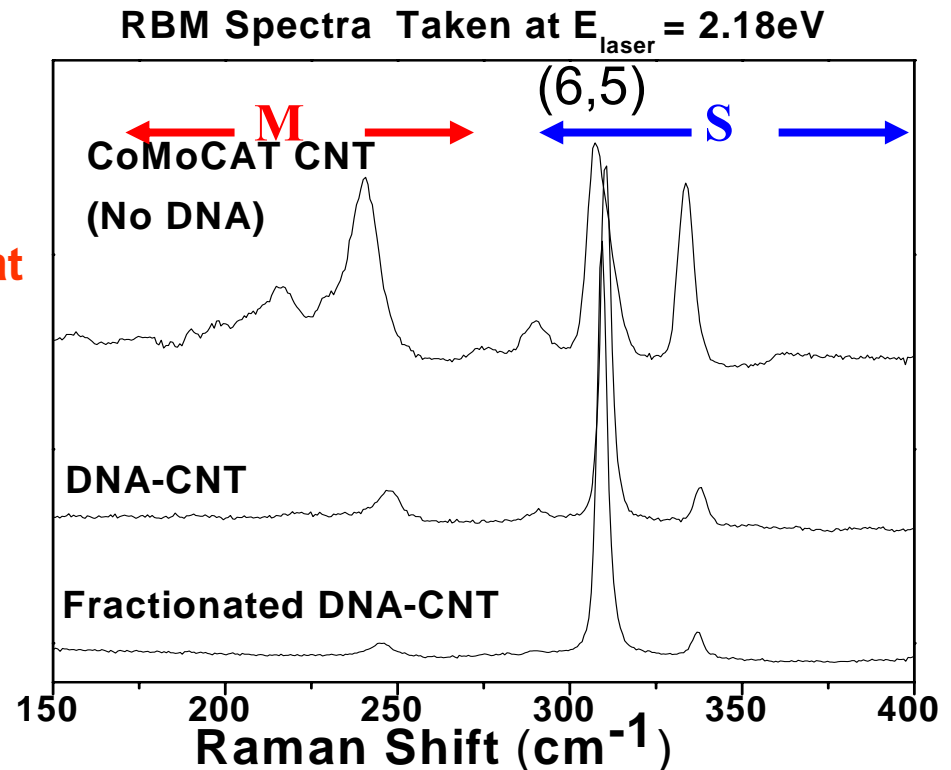
Ion-exchange chromatography (IEC)

Hybrid DNA-SWNTs:

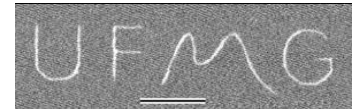
- **M-SWNT** different surface charge density, higher polarizability, elute before S-CNTs

Raman characterization shows that

- DNA wrapping removes metallic (M) SWNTs
- Chromatography further removes M SWNTs preferentially

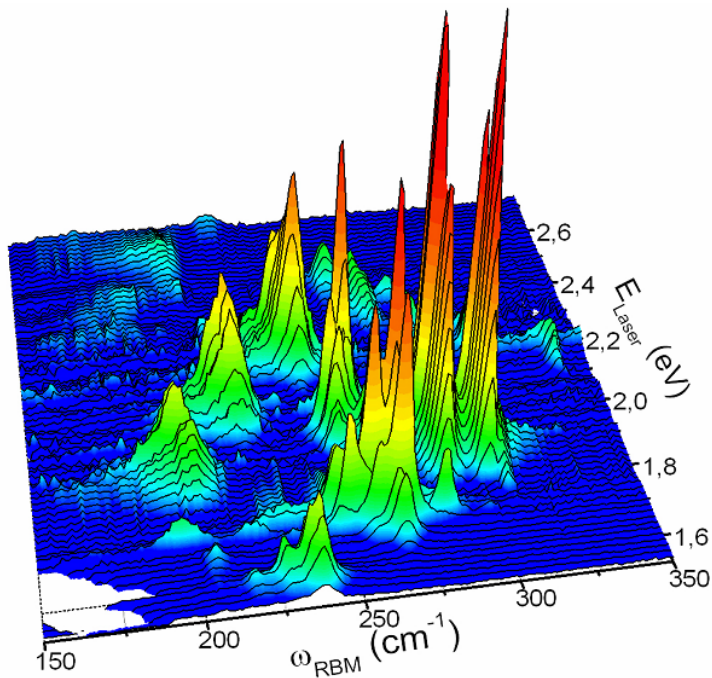
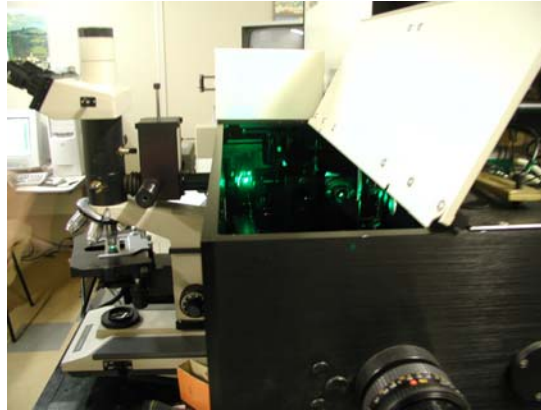


Resonant Raman Spectroscopy Laboratory



- Triple monochromator with optical microscope
- Ar-Kr laser and Ar laser
- Tunable laser systems (Dye-and Ti:Sapphire)

1.5 – 2.7 eV

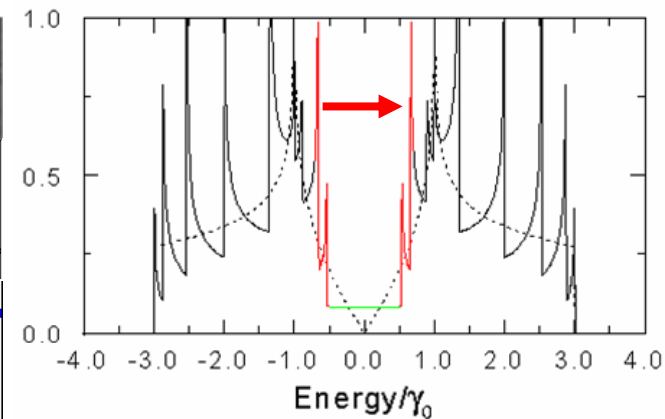
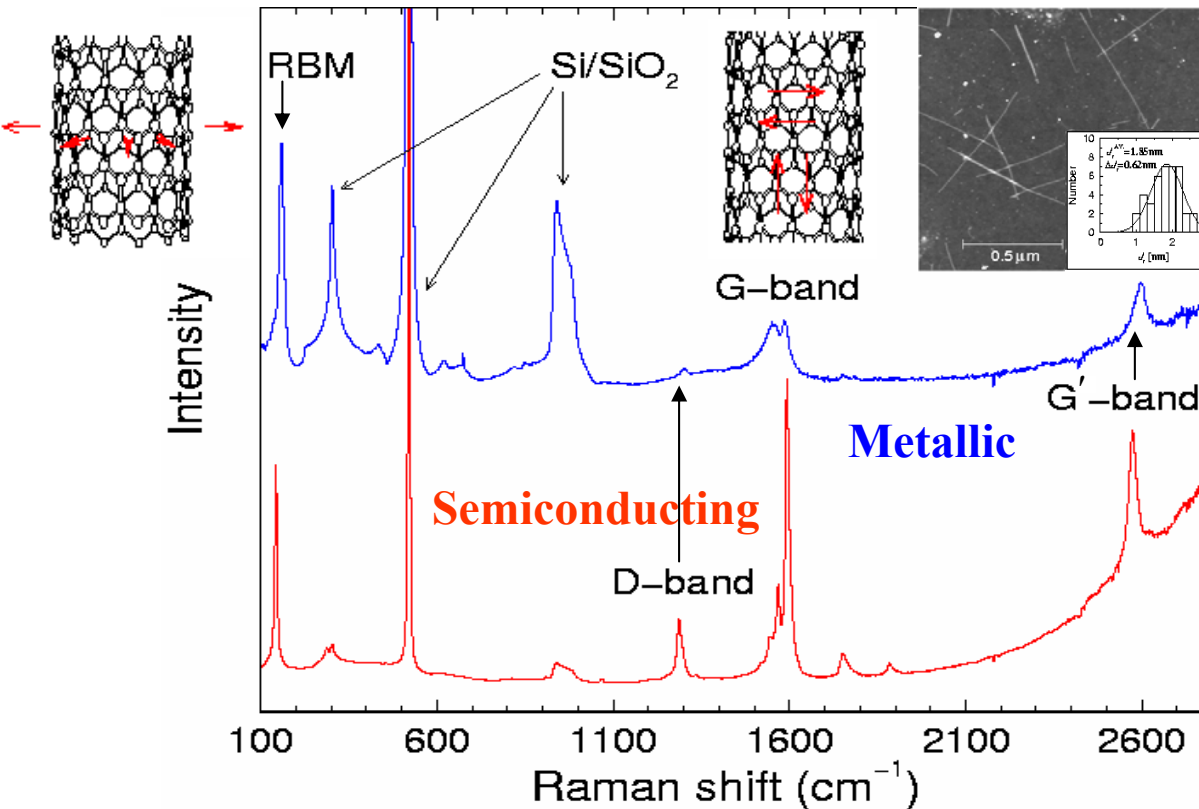


Single Nanotube Spectroscopy yields E_{ii} , (n,m)

Resonant Raman spectra for isolated single-wall carbon nanotubes grown on Si/SiO₂ substrate by the CVD method

A. Jorio et al., Phys. Rev. Lett. 86, 1118 (2001)

RBM



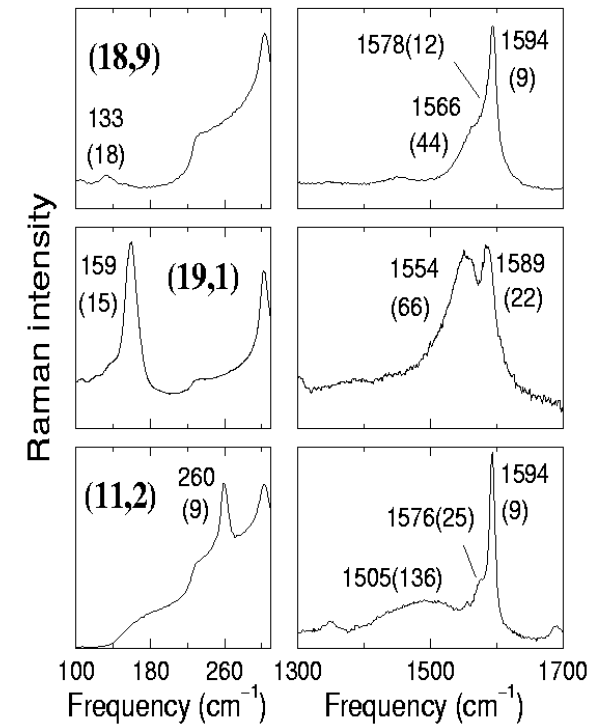
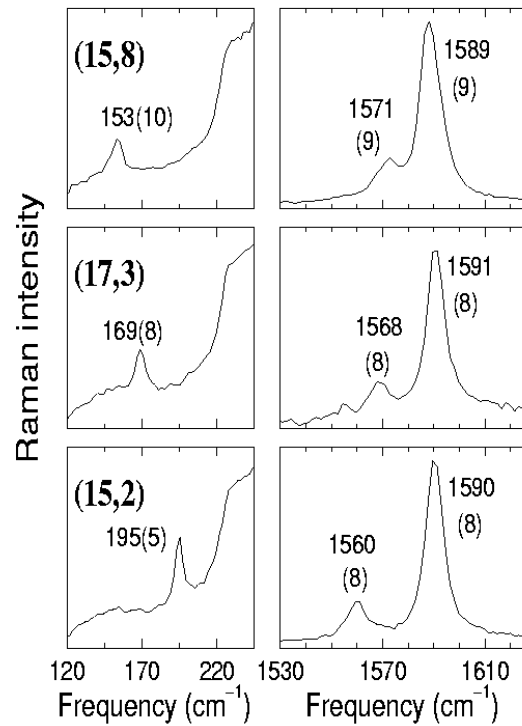
Each nanotube has a unique DOS because of trigonal warping effects *R. Saito et al., Phys. Rev. B 61, 2981 (2000)*

Raman signal from *one* SWNT indicates a strong resonance process

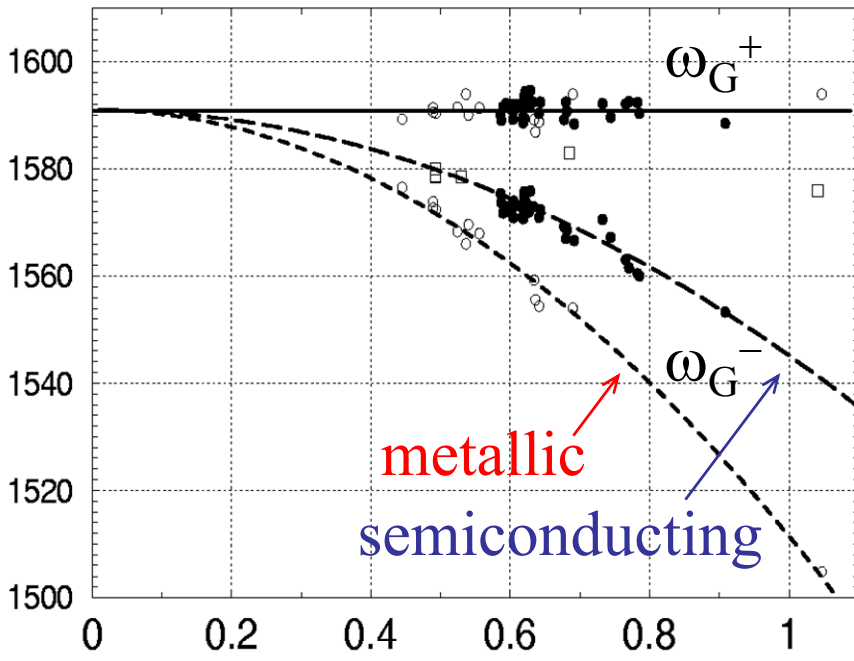
$$(\omega_{\text{RBM}}, E_{ii}) \rightarrow (n,m)$$

G-band frequency dependence on tube diameter

A. Jorio (UFMG) *et al.*,
Phys. Rev. B
 65, 155412 (2002)



Frequency (cm^{-1})



RBM G band
Semiconducting

RBM G band
Metallic

$$\omega_G^+ \sim 1591 \text{ cm}^{-1}$$

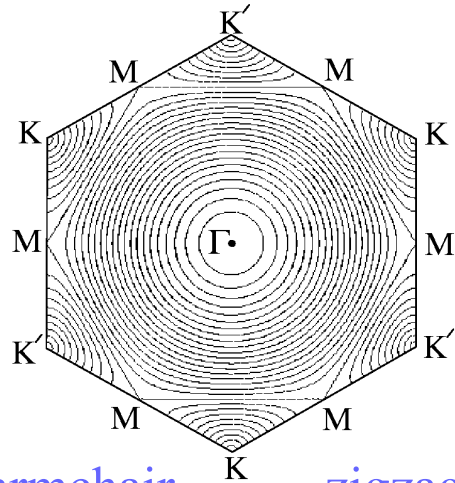
$$\omega_G^- = \omega_G^+ - C/d_t^2$$

$$C_S = 47.7 \text{ cm}^{-1} \text{ nm}^2$$

$$C_M = 79.5 \text{ cm}^{-1} \text{ nm}^2$$

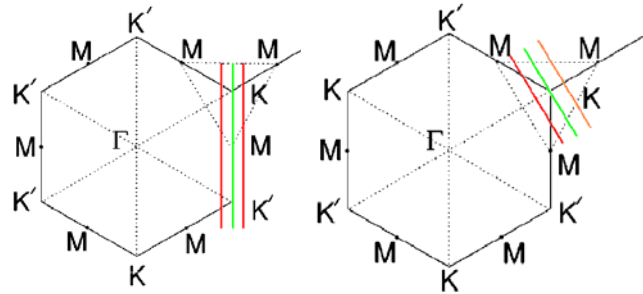
Trigonal Warping Effect in Carbon Nanotubes

R. Saito *et al.*, PRB
61, 2981 (2000)



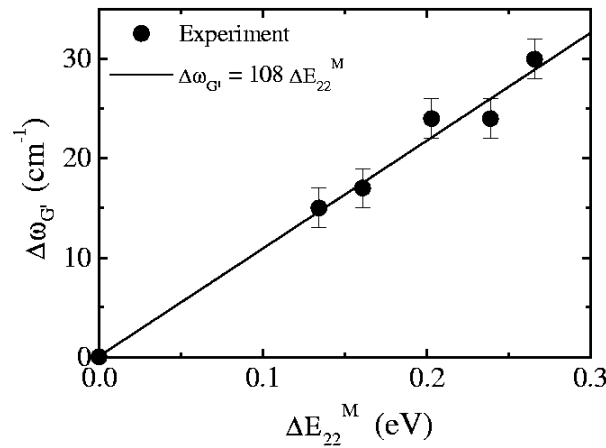
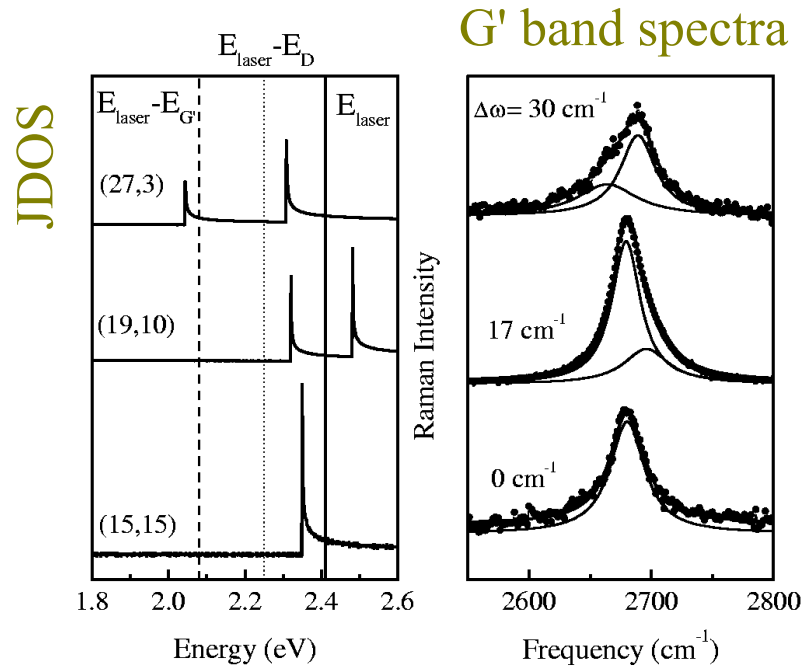
armchair

zigzag

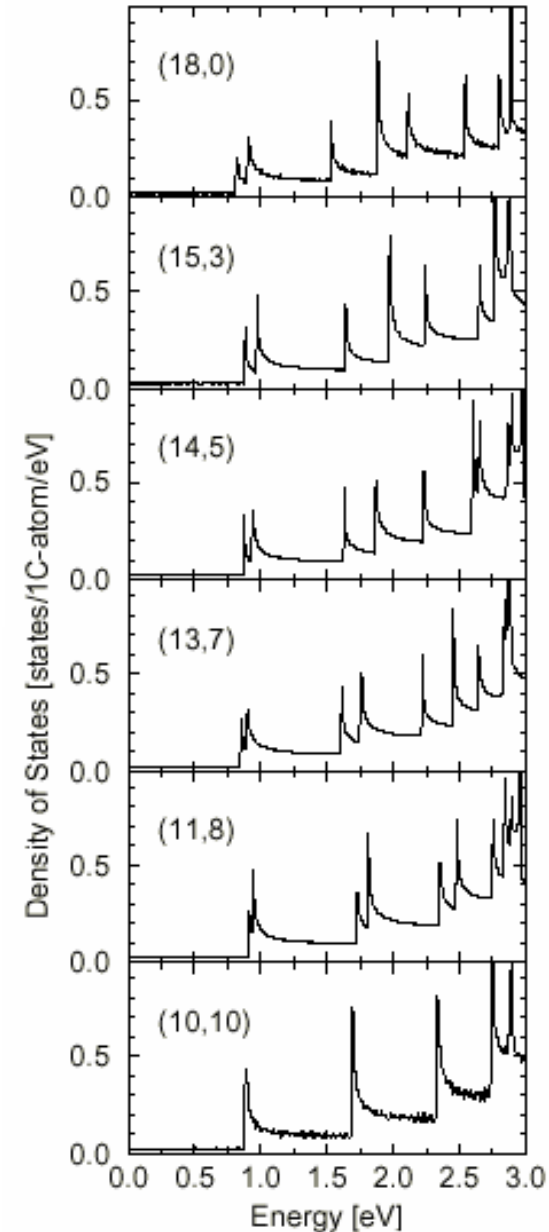


A. G. Souza Filho *et al.*,
CPL 354, 62 (2002)

Allows measurement of splitting of E_{11}^M
For metallic tubes into E_{11L}^M and E_{11H}^M



Splitting of the vHs
in **metallic** SWNTs

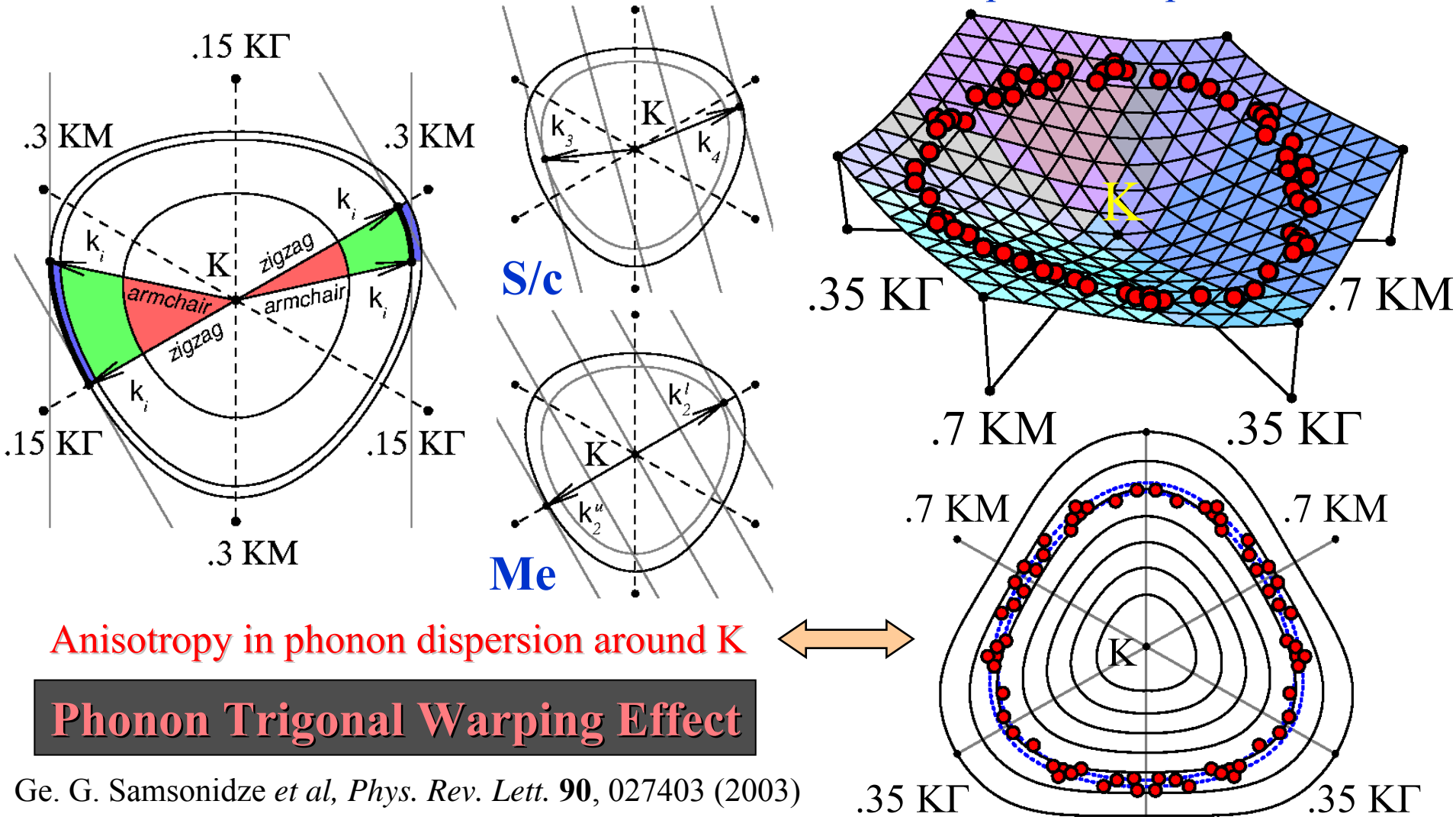


G'-band allows mapping of trigonal warping effect for phonons

2D Graphite — Double Resonance is selective of the wavevector **magnitude**

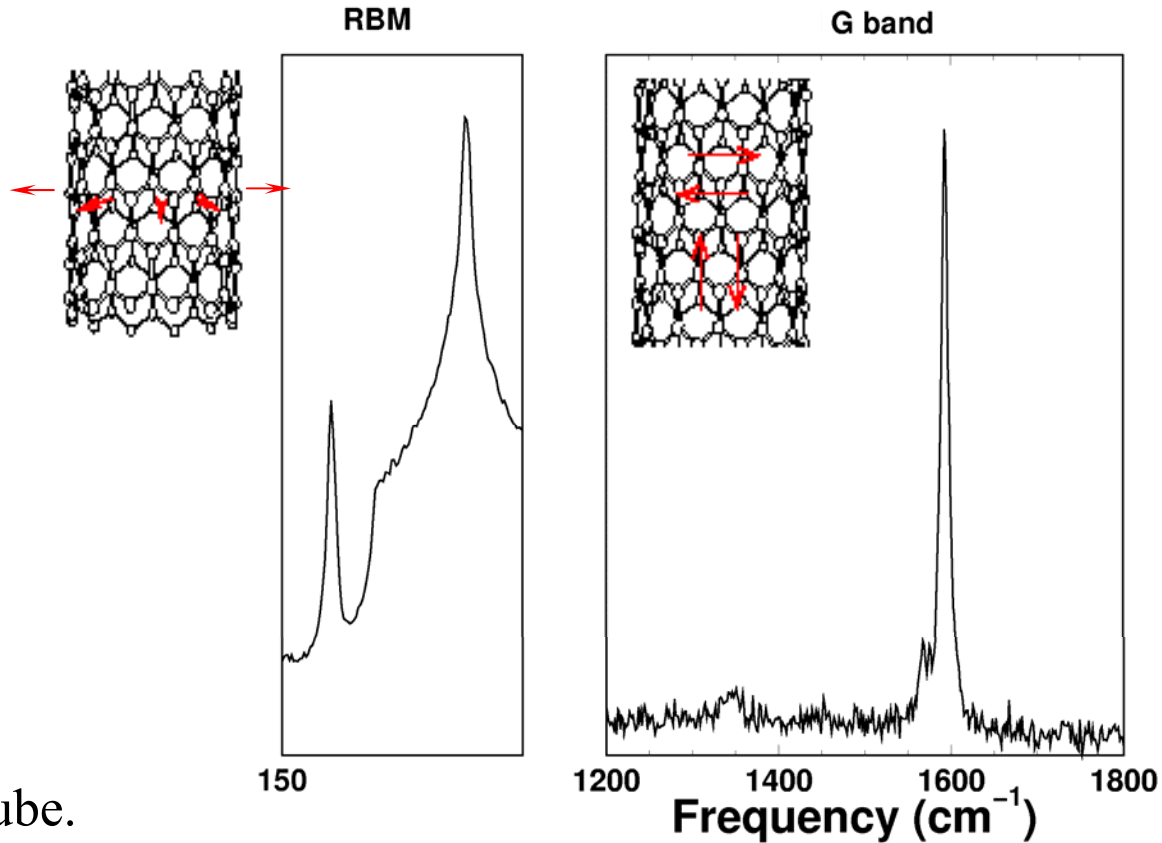
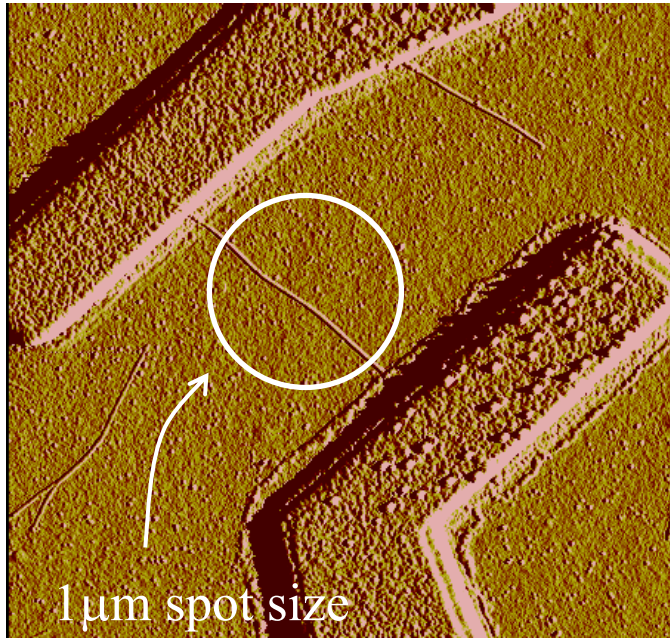
1D SWNTs — Double Resonance is selective of both **magnitude** and **direction**
magnitude – laser energy (2D&1D), direction – chirality (1D)

Quantum confinement — wavevector direction Fit of the phonon dispersion around K



Raman Spectra and Transport for One SWNT

New Research Directions for RRS

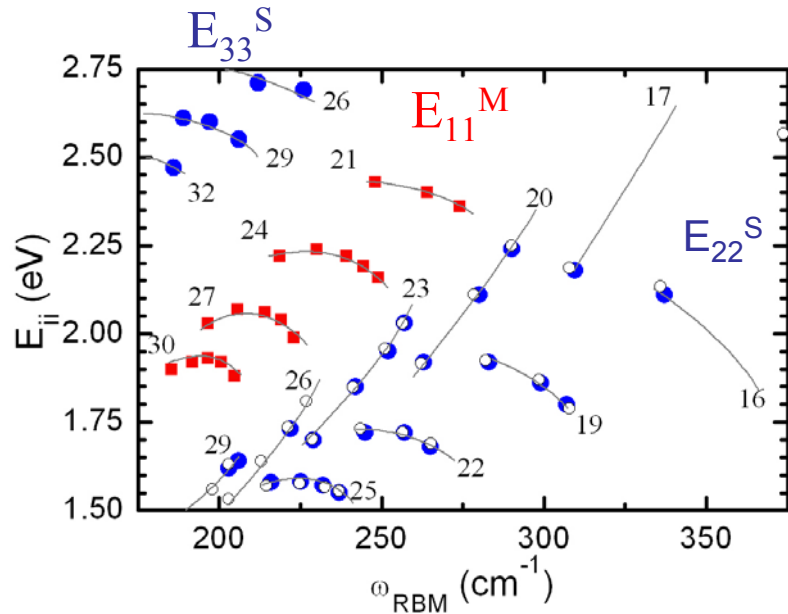


- AFM $d_t = 1-2\text{nm}$ \Rightarrow single tube.
- No voltage applied to sample during Raman Spectroscopy.

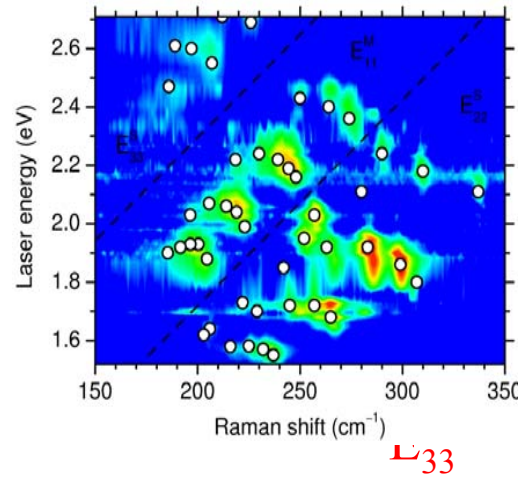
$$\omega_{\text{RBM}} = \frac{248}{d_t}$$

$$\omega_{\text{RBM}} = 185 \text{ cm}^{-1} \Rightarrow d_t = 1.34 \text{ nm}$$

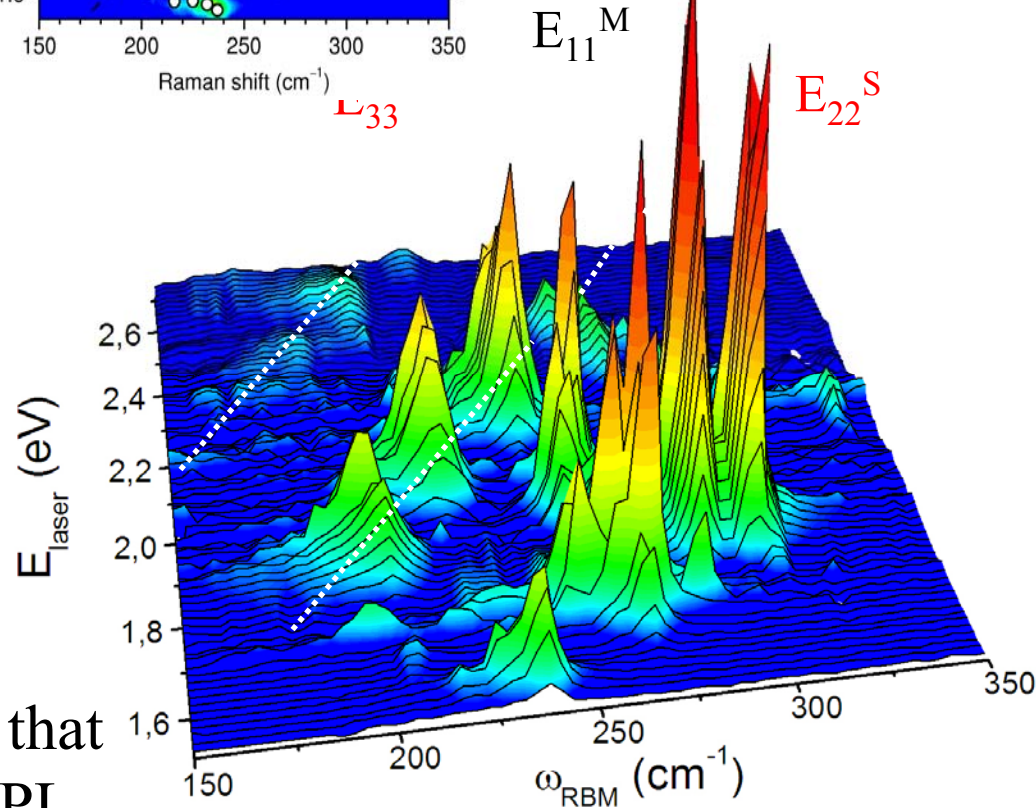
Resonance Raman Spectroscopy on the same sample used for PL



RRS



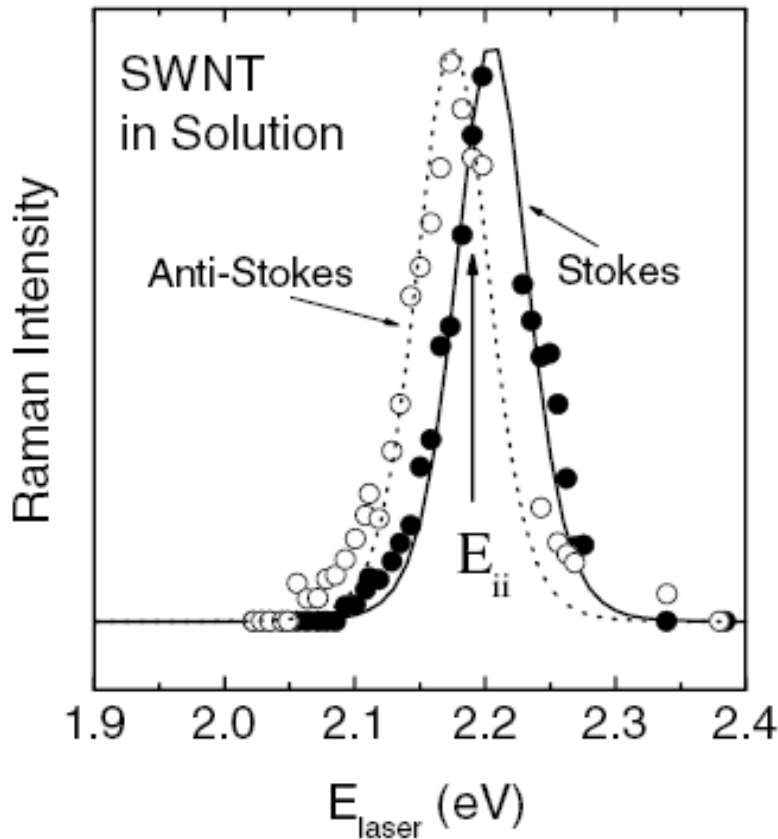
Fantini et al. PRL (2004) showed RRS and PL give the same E_{ii}



Family effect $2n+m=\text{constant}$

Mapping of RRS led to result that E_{ii} is the same for RRS and PL

The Resonance Raman Scattering (RRS) Maps



$$I(E_{\text{laser}}) \propto \left| \frac{1}{(E_{\text{laser}} - E_{ii} - i\Gamma)(E_{\text{laser}} \pm E_{\text{ph}} - E_{ii} - i\Gamma)} \right|^2$$

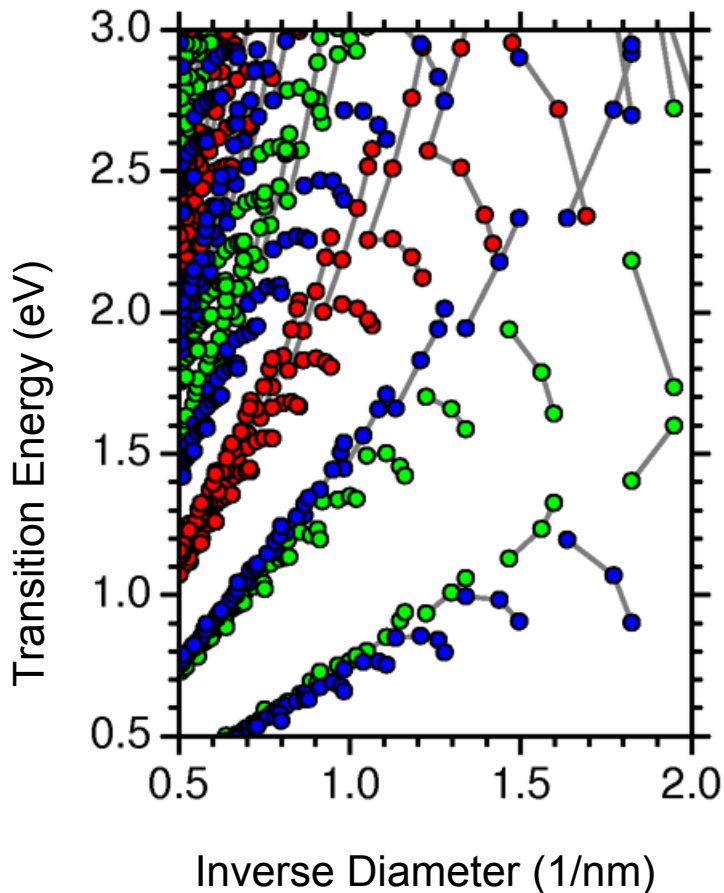
The Raman map for a given ω_{RBM} allows determination of the resonance window for a given (n,m) tube. Measurement of the Stokes and anti-Stokes profiles gives transition energy E_{ii}

$$\omega_{\text{RBM}} (cm^{-1}) = \frac{219}{d_T (nm)} + 15$$

C. Fantini et al., Phys. Rev. Letters, 93, 147406 (2004)

$$(E_{ii}, \omega_{\text{RBM}}) \rightarrow (n,m)$$

EXTENDED TIGHT BINDING (ETB)



M

S1 $2n+m=3p+1$

S2 $2n+m=3p+2$

Kataura plot is calculated within the extended tight-binding approximation using Popov/Porezag approach:

- ❖ curvature effects ($ss\sigma$, $sp\sigma$, $pp\sigma$, $pp\pi$)
- ❖ long-range interactions (up to $\sim 4\text{\AA}$)
- ❖ geometrical structure optimization

The extended tight-binding calculations show family behavior (differentiation between S1 & S2 and strong chirality dependence) similar to that of PL empirical fit

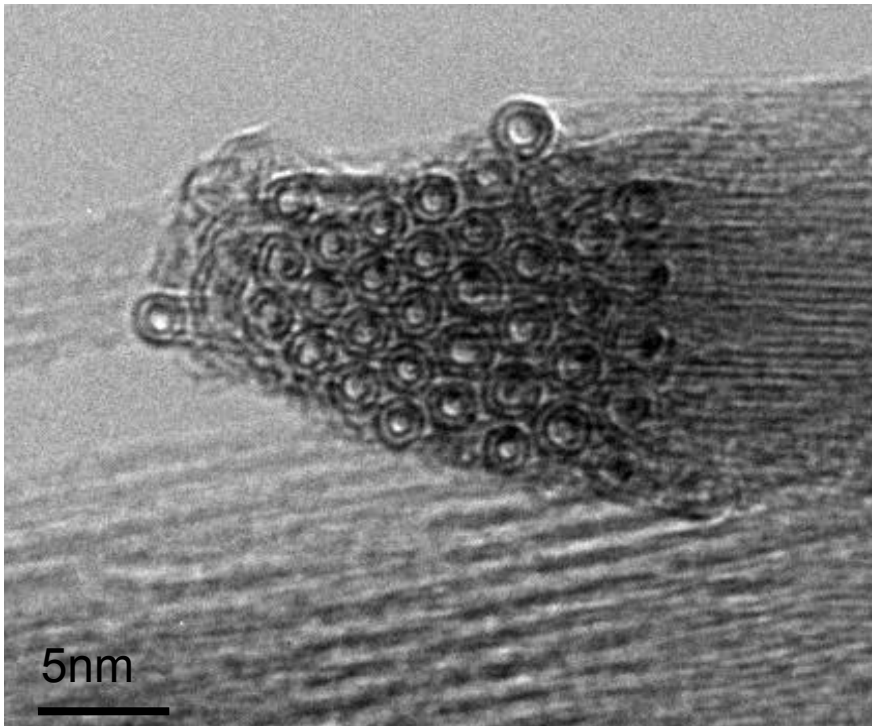
ETB model is widely used for characterization of carbon nanotubes

Ge.G. Samsonidze et al., APL 85, 5703 (2004)

Popov et al. Nano Lett. 4, 1795 (2004) & New J. Phys 6, 17 (2004)

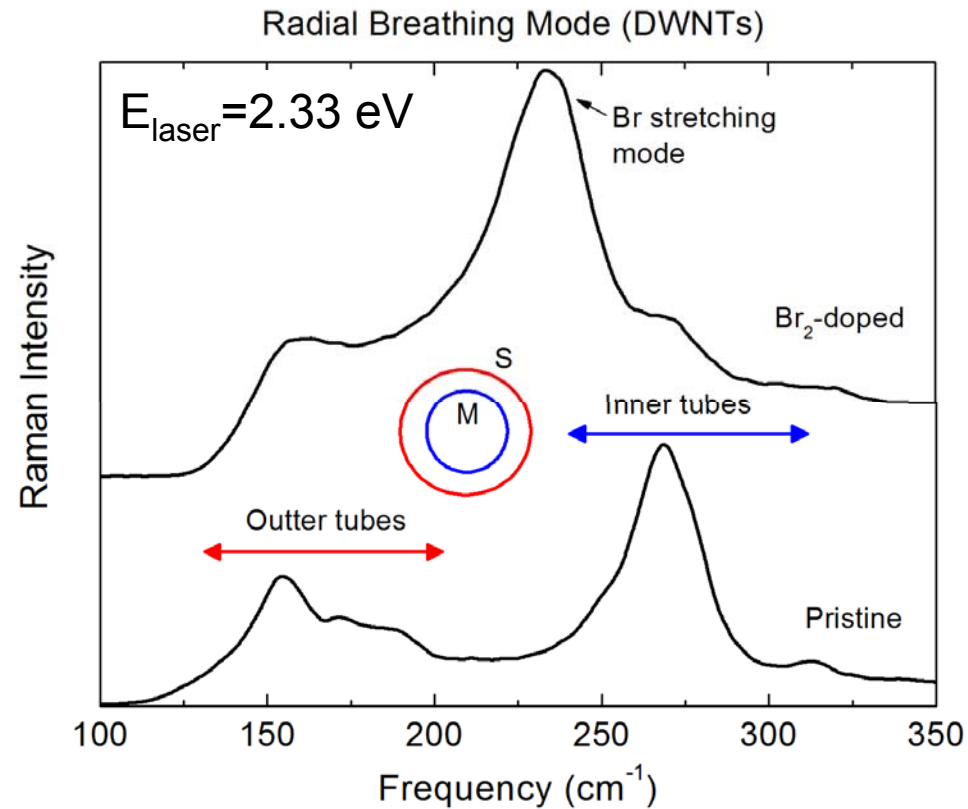
Br₂-doped double-wall nanotubes

Highly pure samples



M. Endo (Japan)

A. G. Souza Filho et al. (2006)

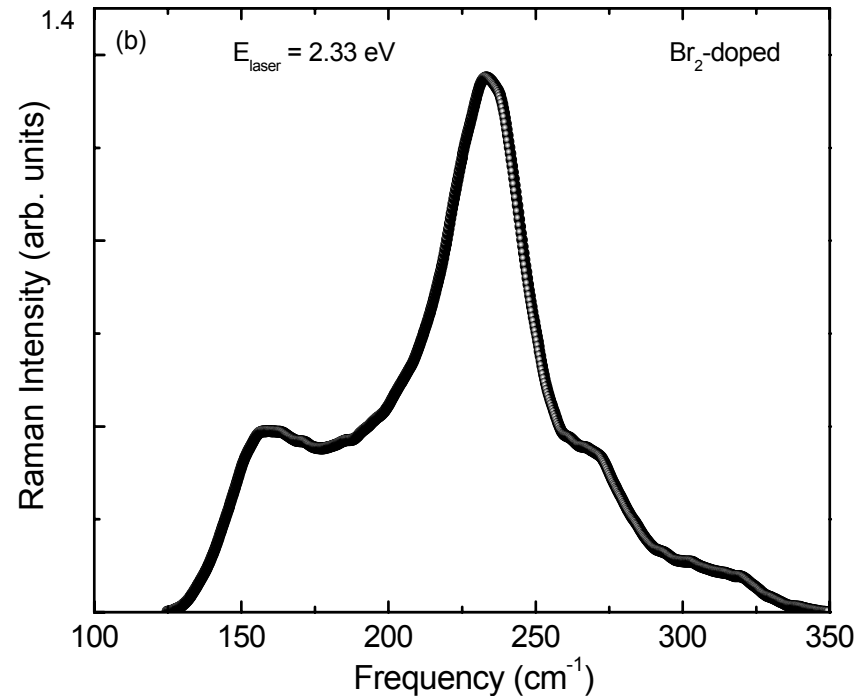
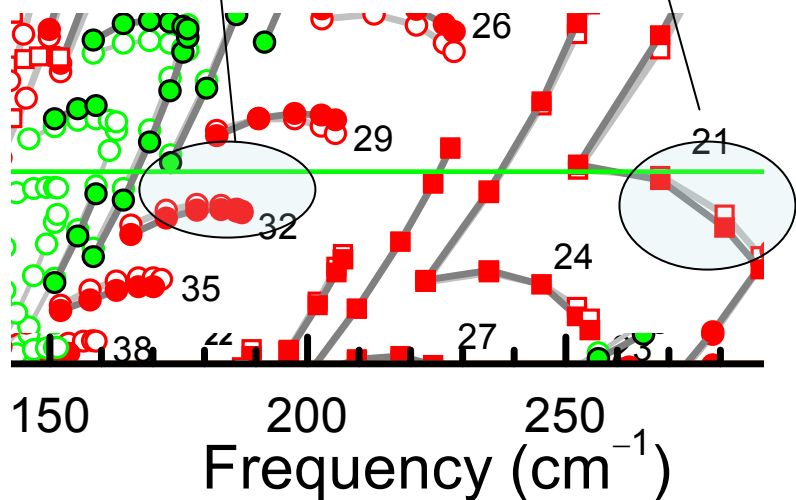
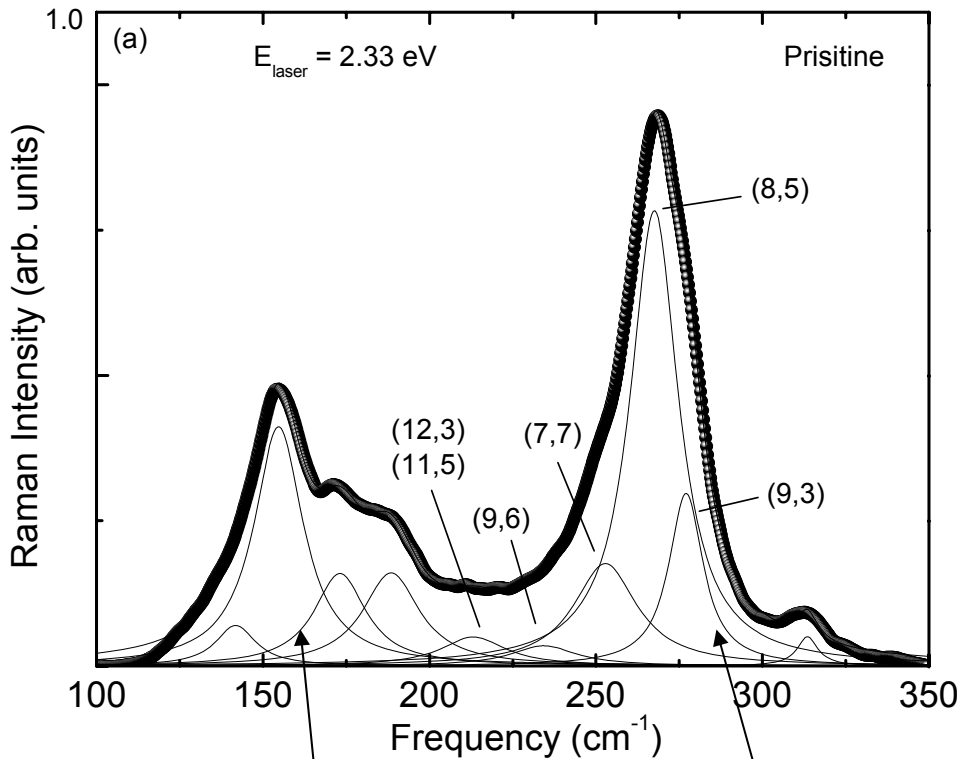


- Different configuration outer/inner tubes depending on laser energy,
- The Raman spectrum of the dopant and of the host

Semiconducting inner/Metallic outer configuration

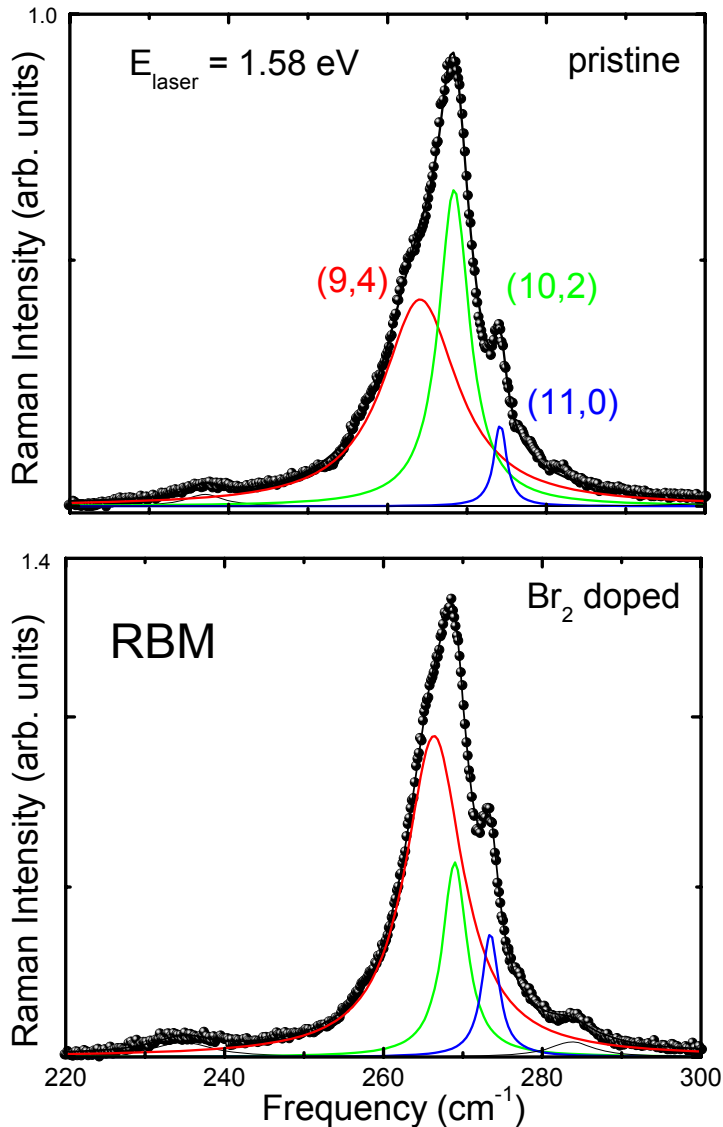
RBM properties at $E_{\text{laser}}=2.33$ eV

- The effect of intercalation on individual inner (n,m) tubes can be studied.
- Spectrum from both the nanotubes and the dopant

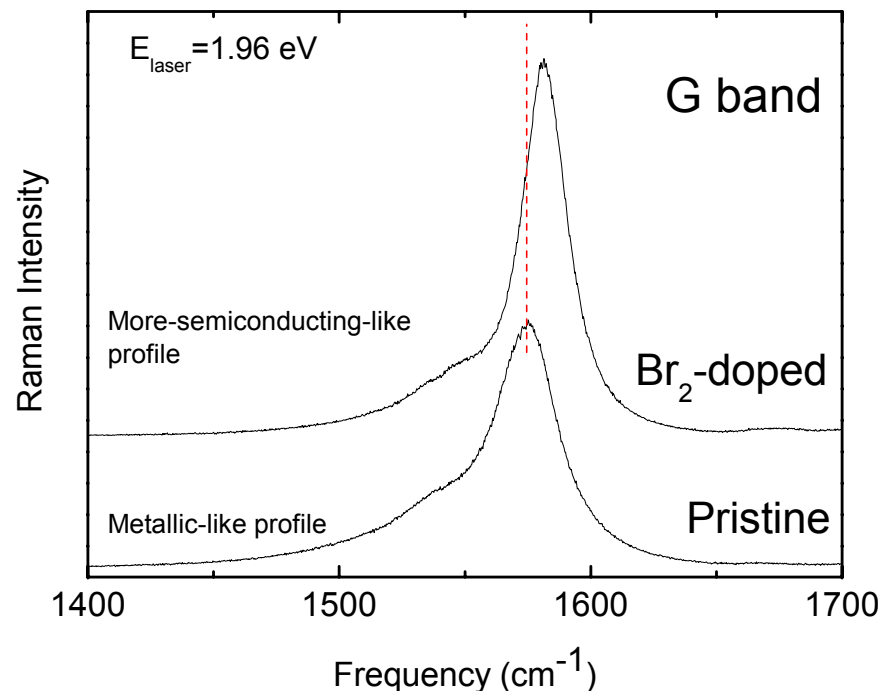


Souza Filho et al PRB (2006)

Doping effects: changes in the Fermi level and electronic transitions E_{ij} values



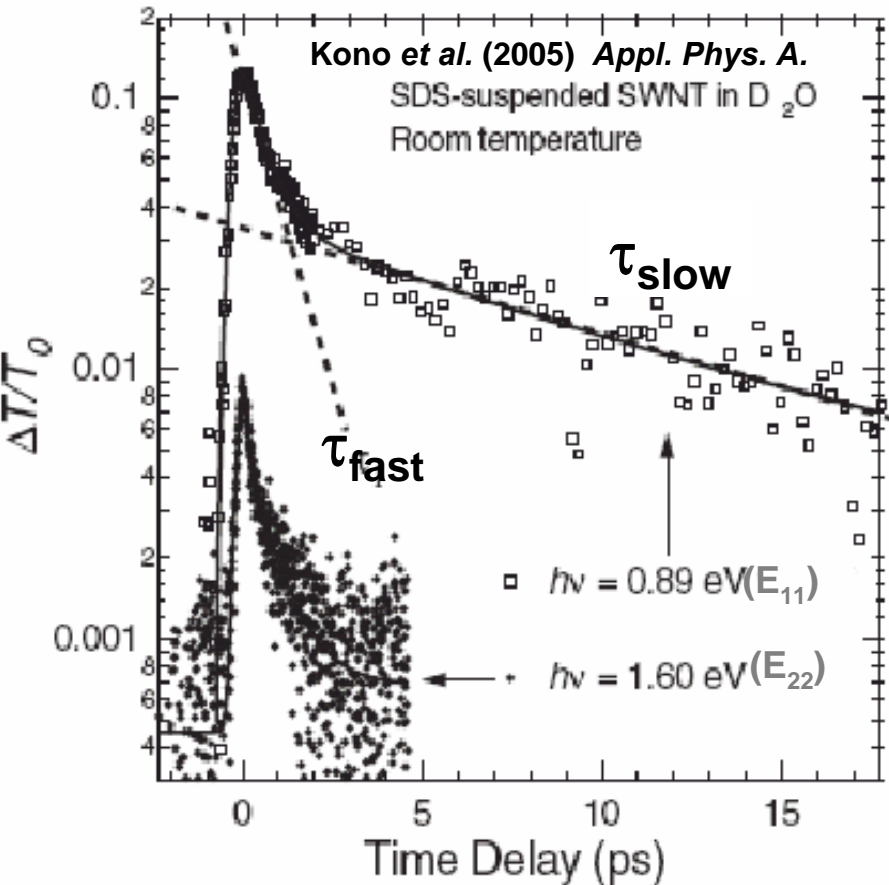
- Changes in the relative intensities indicate Changes in E_{ij} values
- Upshifts observed in the G band indicate Charge transfer and changes in the E_F .
- Br₂ is acting as an acceptor
- Intercalation of nanotubes is complementary to that of graphite but shows unique aspects



Outline on Characterization with a Focus on optical characterization

- **What is in my sample?**
- **What we can learn from:**
 - **Photoluminescence?**
 - **Raman spectroscopy?**
 - **Fast Optics?**

Pump-Probe Studies with Fast Optics



Pump-Probe Studies:

- Pump-Probe at the band edge

• Transient Spectrum:

- Single or biexponential decay
(Hertel *et al.* Nano. Lett., 2004)

Slow Component, τ_{slow} :

- 10-180ps,
- Radiative relaxation from band edge

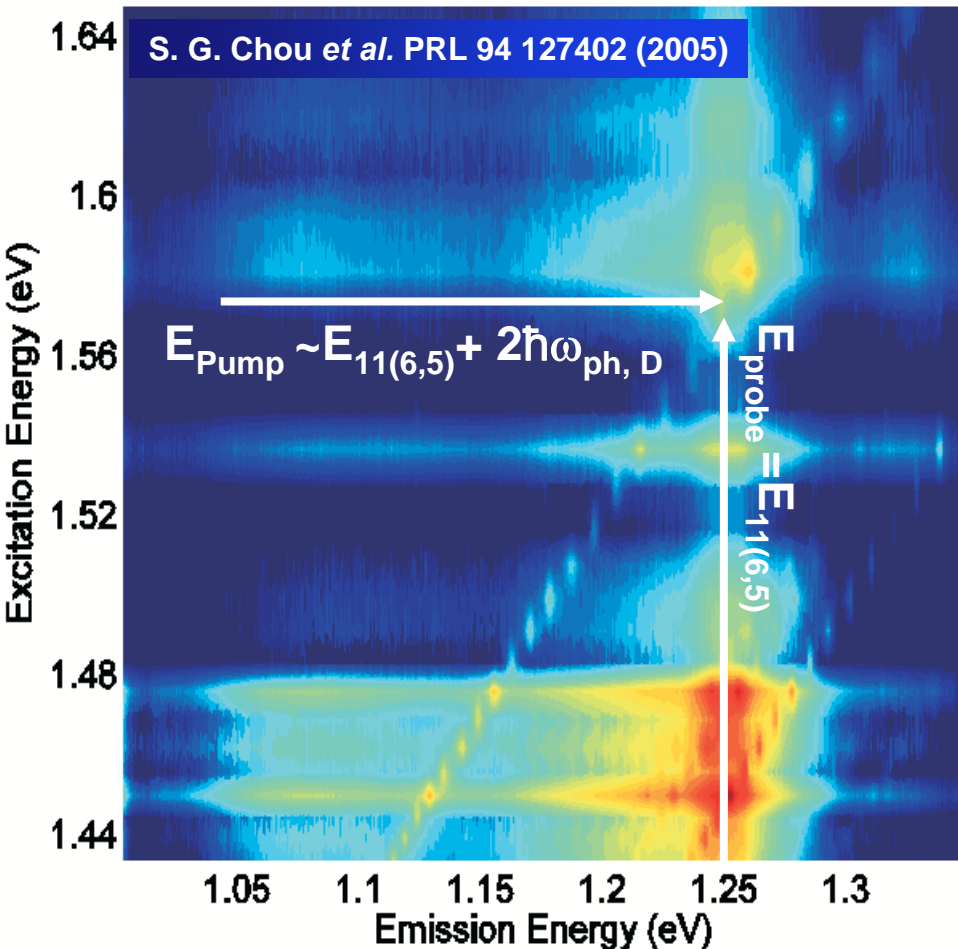
• Fast component, τ_{fast} :

- 100-900fs, Intraband relaxation
- Rapid internal thermalization via
- electron-electron scattering.
Gives reason for low PL intensity

(Hagan *et al.* Appl. Phys. A. (2005))

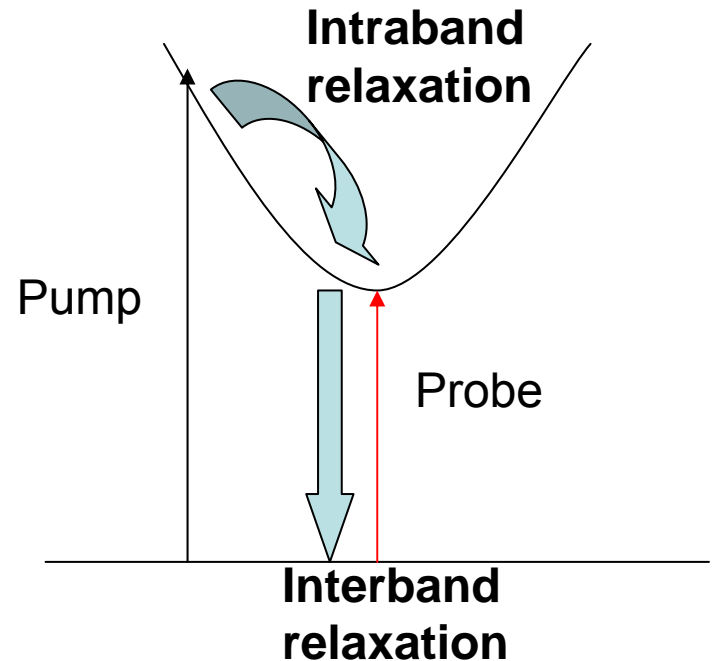
Non-degenerate Pump-Probe

Frequency domain



Fast optics, Time domain

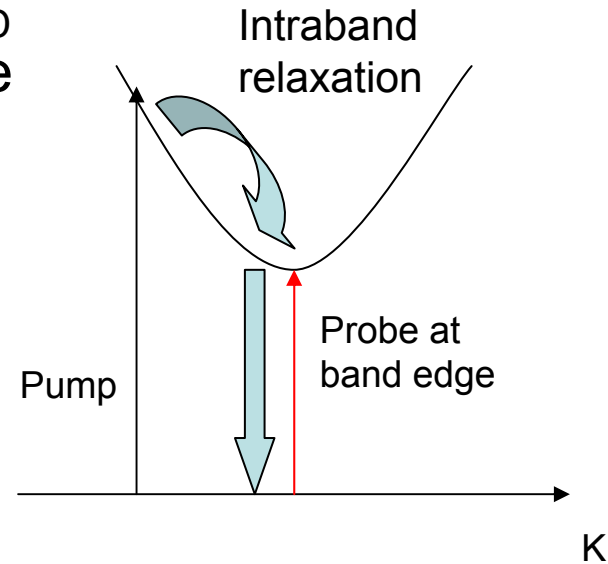
$E_{\text{pump}} = 1.57 \pm 0.01 \text{ eV}, \sim E_{11}(6,5) + 2\hbar\omega_{\text{D}}$
 $E_{\text{probe}} = \text{around } E_{11} \text{ of } (6,5) \text{ nanotube}$
(Instrument resolution $\sim 250\text{fs}$)



S. G. Chou *et al.* (unpublished)

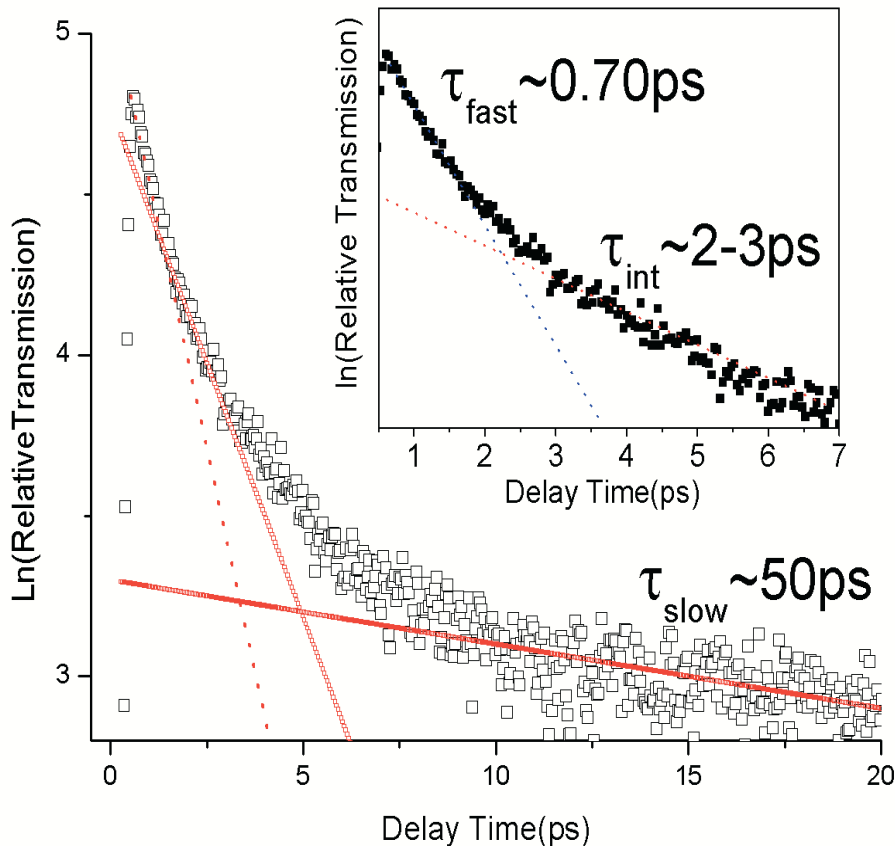
Pump Probe Studies at Special E_{pump}

- $E_{\text{pump}} = 1.57 \pm 0.01 \text{ eV} \approx E_{11}^{1A- (6,5)} + 2\hbar\omega_D$
- $E_{\text{probe}} = \text{around } E_{11}^{1A-} \text{ of } (6,5) \text{ nanotube}$

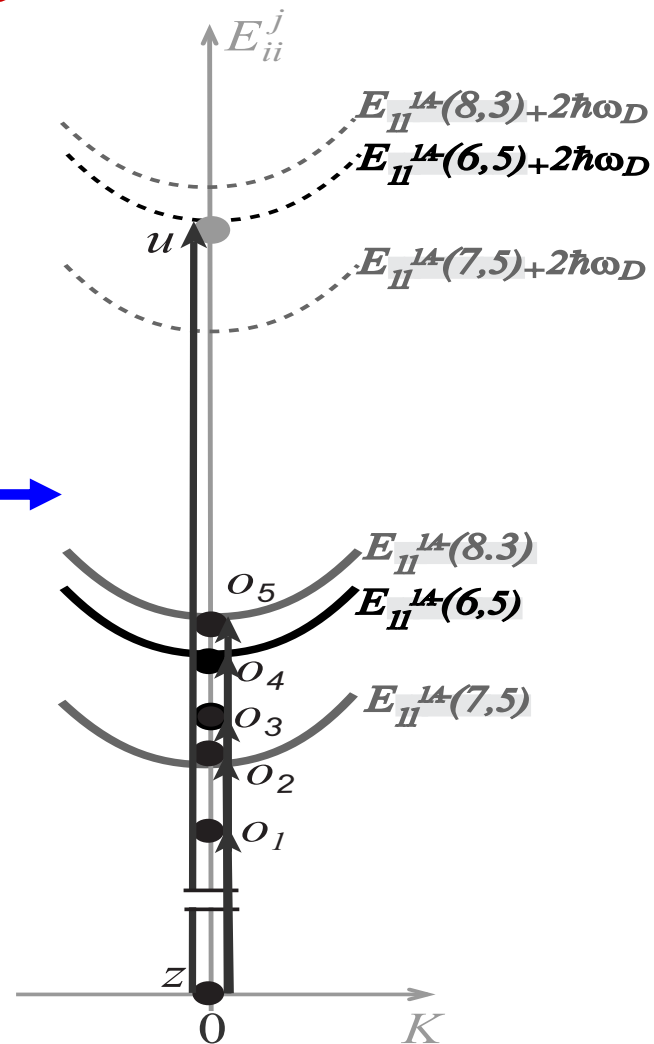
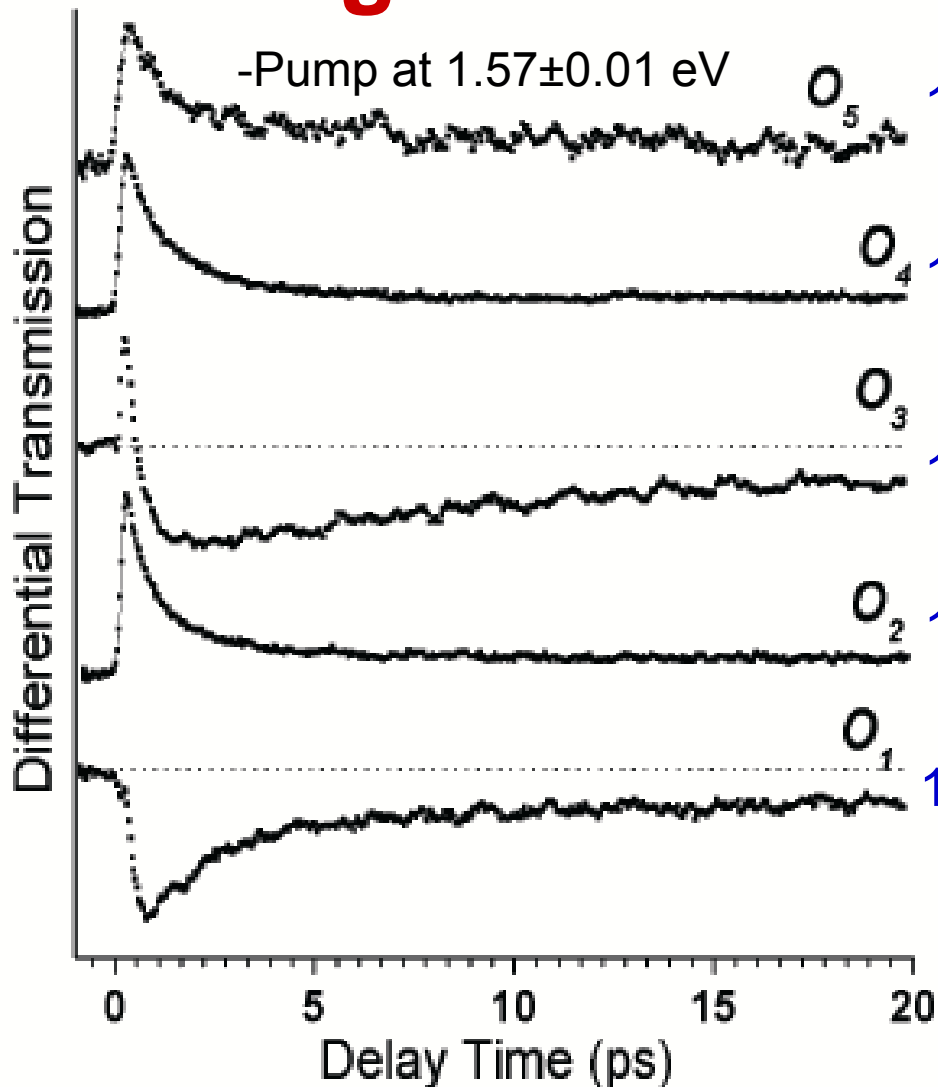


Exciton population at $E_{11}^{1A- (6,5)}$:

- Quick rise (within 200fs)
- Three decay components:
 - $\tau_{\text{fast}} \sim 680 \text{ fs}$ (dominant process)
 - $\tau_{\text{int}} \sim 2\text{-}3 \text{ ps}$ (dominant process)
 - $\tau_{\text{slow}} \sim 50 \text{ ps}$ (weak during first 20ps).



Probing at Different Energies:



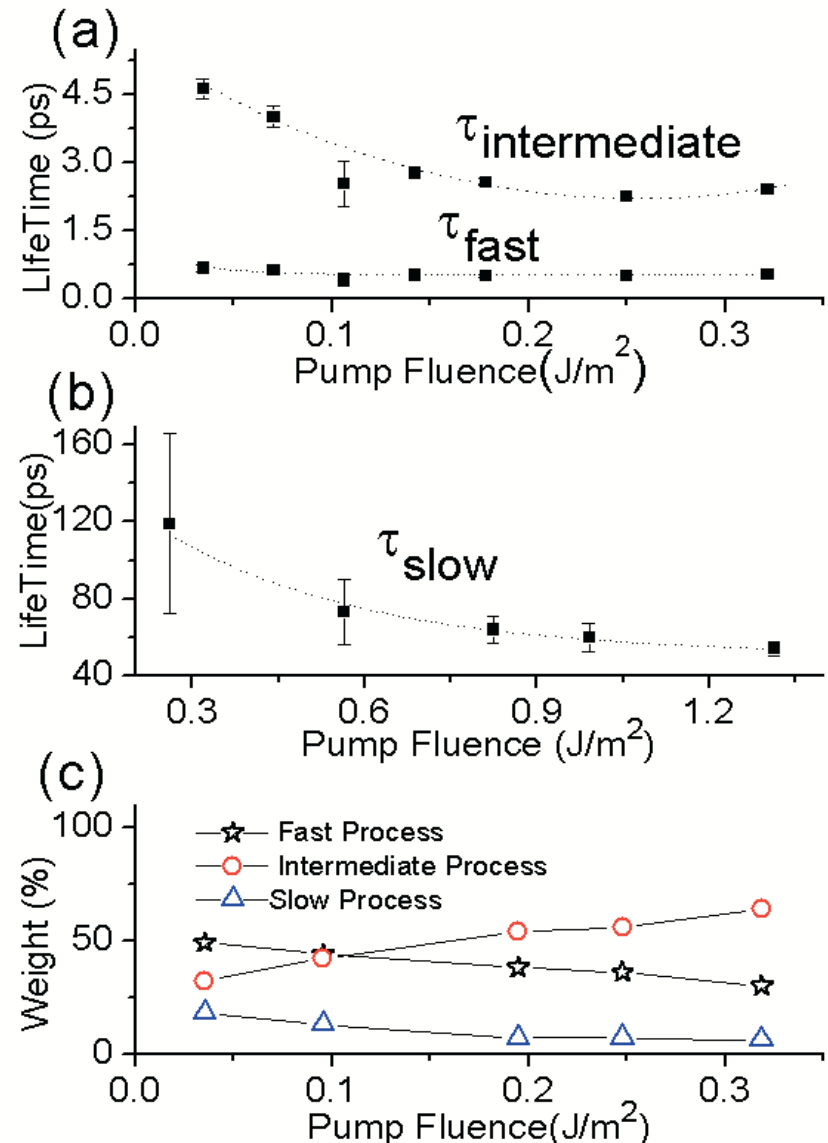
Exp.	(n,m)	E_{Probe}	Fluence J/m^2	fast	%	Int	%	Slow	%
O_5	(8,3)	1.27eV	0.3	900fs	70	Several ps	Traces mixed	30ps	30
O_4	(6,5)	1.25eV	0.3	700fs	45	3ps	45	50ps	10
O_2	(7,5)	1.20eV	0.1	800fs	90	N/A	N/A	40ps	10

Pump Fluence Dependence

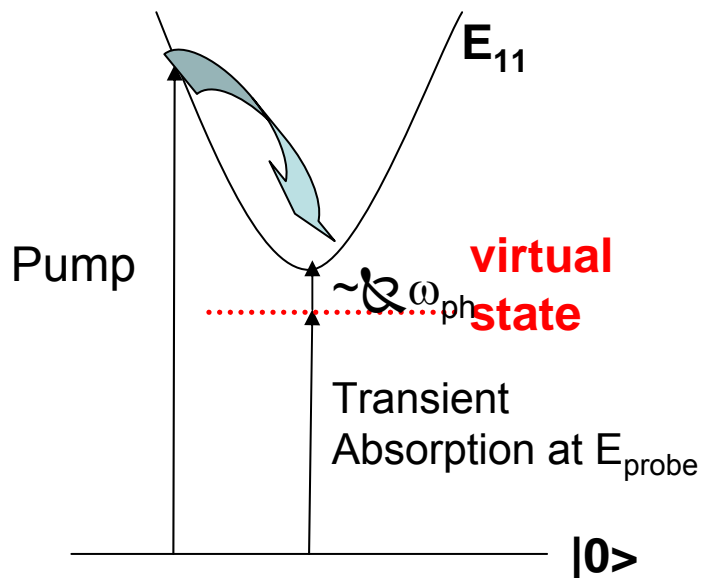
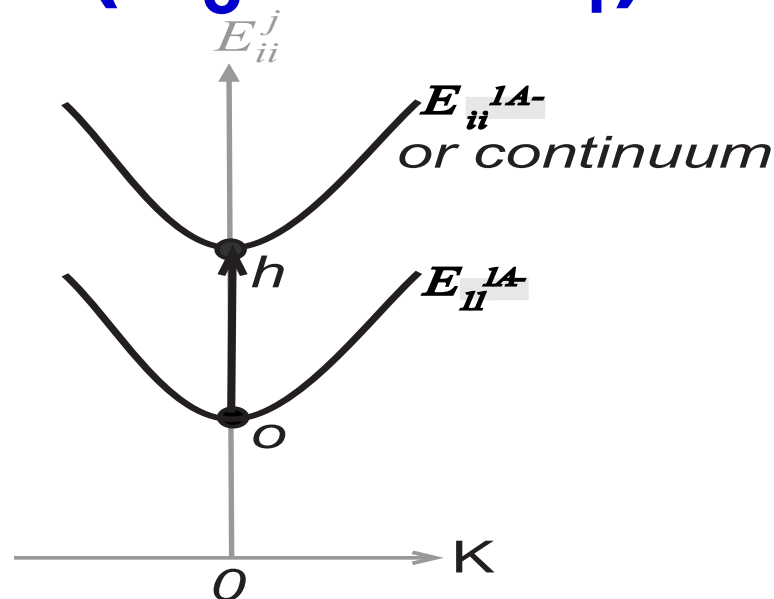
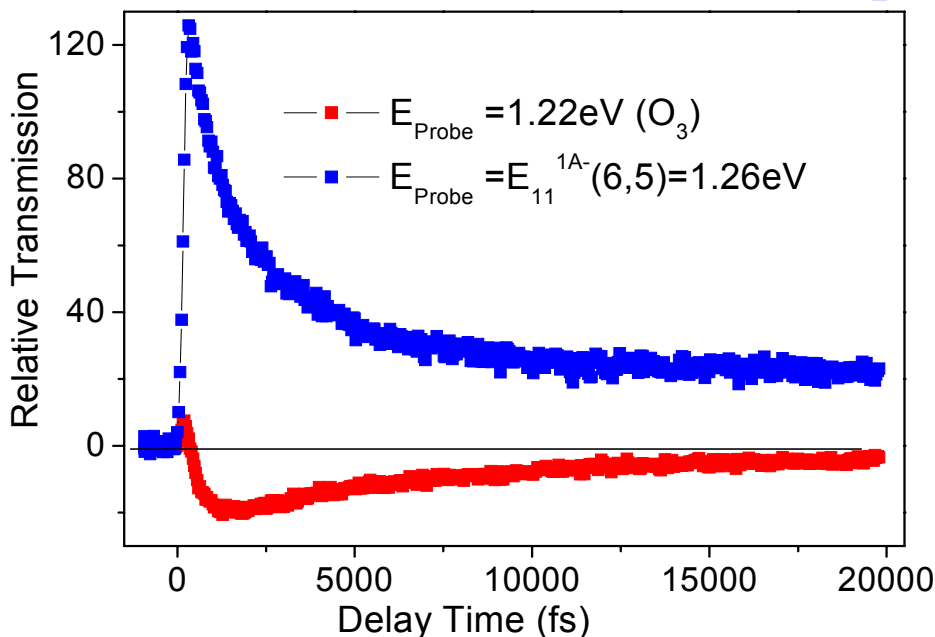
- Probing at $E_{11}^1A^-(6,5)$:

(For B.S. #5)

- Clear pump fluence dependence for τ_{int} and τ_{slow}
- % weight for τ_{int} increases with increasing pump fluence
- Observed fluence dependence can be explained by the proposed decay process for each time scale.



Transient Absorption (O_3 and O_1):



Transient Absorption:

- $DT < 0$ suggests the presence of transient absorption processes.
- Observed previously for probe energies slightly below E_{11} (Yang *et al.* PCCP, 7, 512-517(2005))
- Timescale $\sim 10\text{ps}$
- Phonon absorption from a virtual state. (anti-Stokes processes).

Different Decay Processes

τ_{fast} :

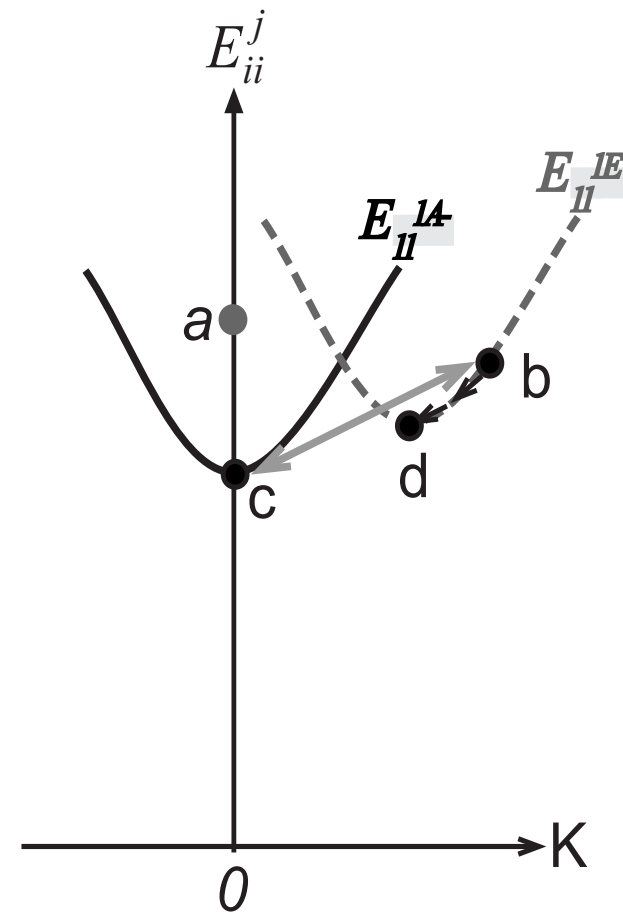
Decay via e-e interactions dominated by Auger process.

τ_{slow} :

non-radiative recombination

τ_{int} :

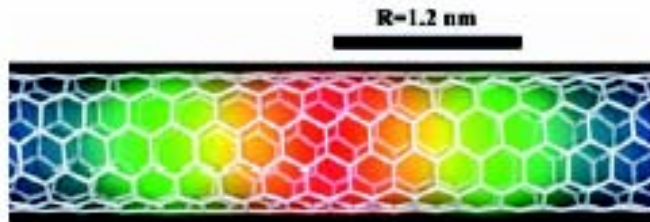
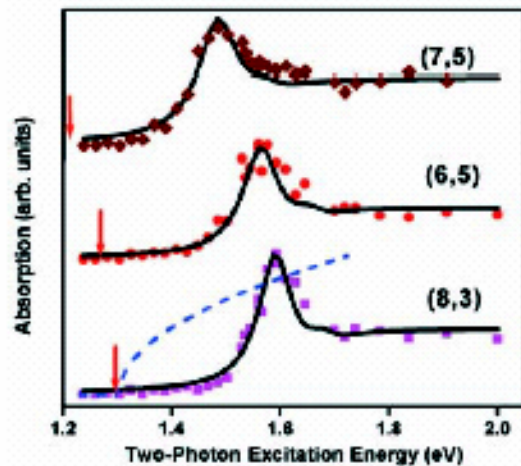
- Exciton population at **c** can be depleted by absorbing a “hot” D-band phonon
- **b** \leftrightarrow **c** process can establish detailed balance and keep exciton population at **c** at an almost steady state.
- Excitons at **b** can also leak into **d** and never return to **c**. Thus, τ_{int} is really the timescale of such a phonon “leaking” process.



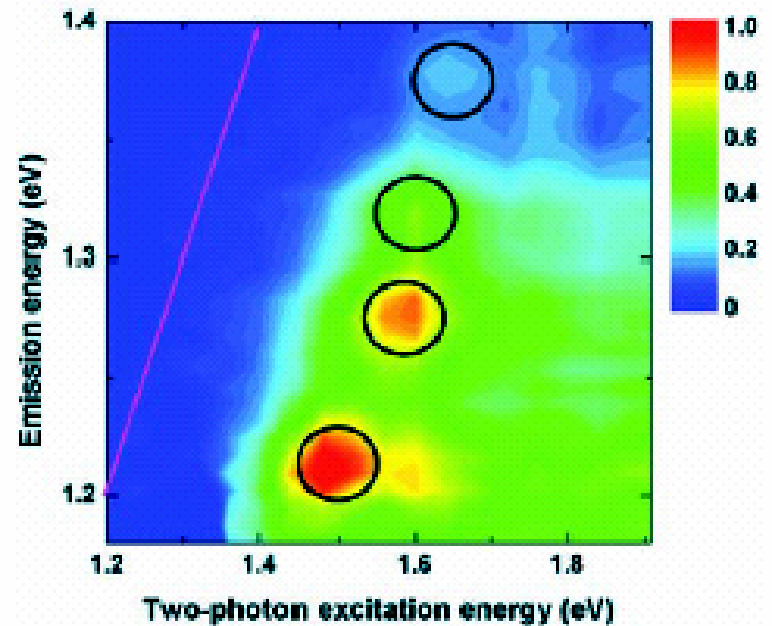
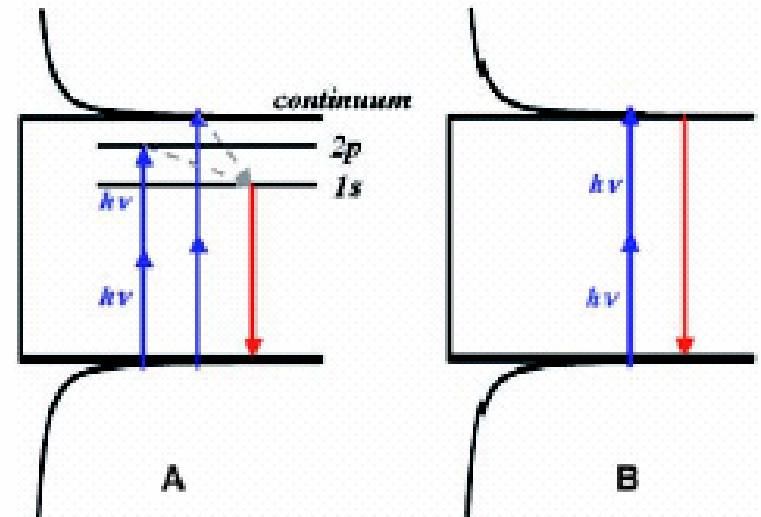
Evidence for excitons in two-photon optical spectroscopy

Wang et al, Science 308, 838 (2005)

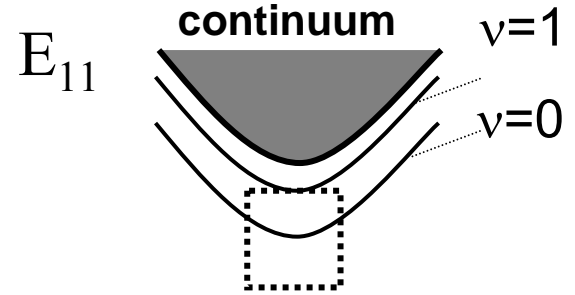
Maultzsch et al PRB 72, 241402 (2005)



Density of the 1s-exciton envelope wave function for a (6,5) SWNT



Symmetry of Excitons in Chiral Tubes



Exciton Symmetry
Effective Mass Approximation

Envelope function

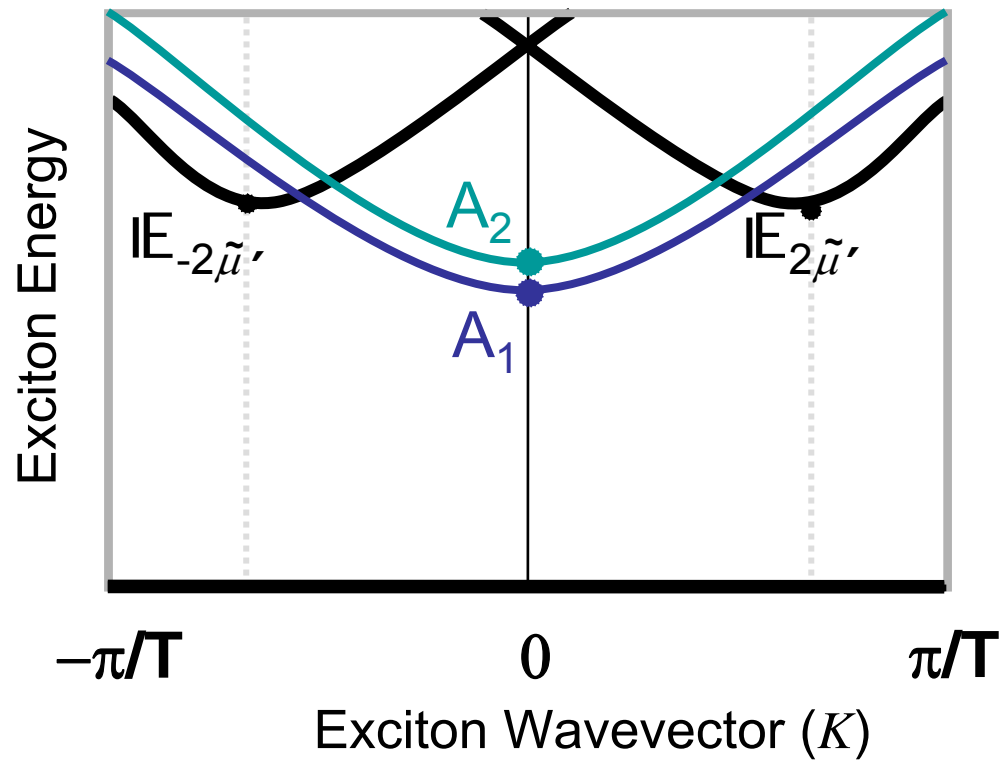
$$\mathcal{D}(\psi^{EMA}) = \underbrace{\mathcal{D}(\phi_c) \otimes \mathcal{D}(\phi_v)}_{\text{Symmetry of the Bloch Function for the exciton}} \otimes \mathcal{D}(F_\nu), \quad \Rightarrow \quad \mathcal{D}(F_\nu) = \begin{cases} A_1 & - \nu \text{ even} \\ A_2 & - \nu \text{ odd} \end{cases}$$

Symmetry of the Bloch Function for the exciton

$$\mathcal{D}(\phi_c) \otimes \mathcal{D}(\phi_v)$$

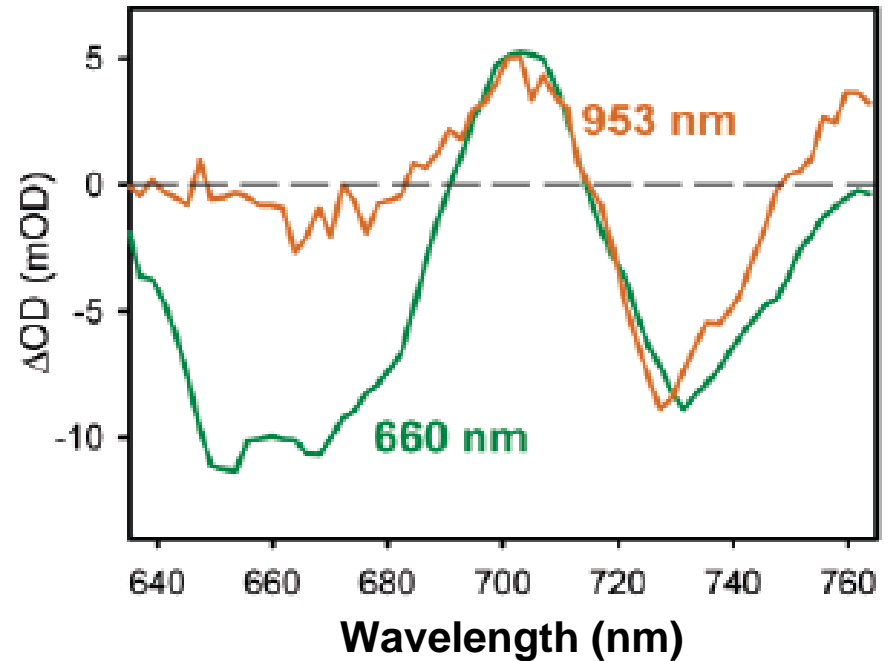
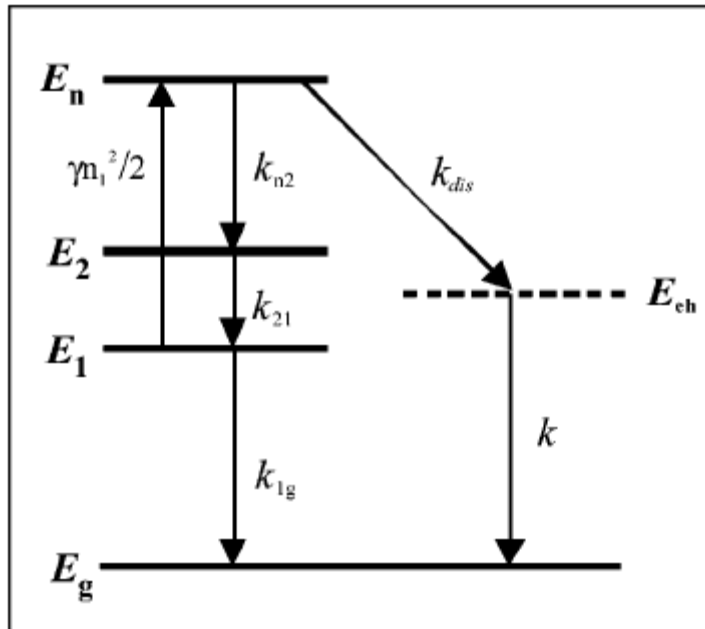
$$A_1 + A_2 + |E_{2\mu} + E_{-2\mu}$$

Both ν even and odd envelope functions have exciton states active for 1-photon (A_2) and 2-photon (A_1) excitation. Therefore two photon absorption depends on magnitude of matrix elements.



Direct Measurement of Exciton Binding Energy by Fast Optics

Y. Ma et al. Phys. Chem B Lett. 109,15671 (2005)



Excitation to either E_1 or E_2 leads to occupation of E_n by an Auger process which relaxes either to E_1 or E_{ch} yielding an exciton binding energy of $(E_{ch}-E_{11}) = 0.41\text{eV}$ for the (8,3) SWNT.

Acknowledgements:

Funding:

- NSF
- DuPont-MIT Alliance

Collaboration with

- UFMG, Brazil
- IPICYT, Mexico
- Tohoku U., Japan
- DuPont
- Boston University

Collaborators

R. Saito	Tohoku Univ., Japan
J. Jiang	Tohoku Univ., Japan
M. Endo	Shinshu Univ., Japan
A. Jorio	Physics, UFMG, Brazil
Ge. G. Samsonidze	EECS, MIT, USA
S. G. Chou	Chemistry, MIT, USA
H. Son	EECS, MIT, USA
J. Kong	ECS, MIT, USA
D. Tokmakoff	Chemistry, MIT, USA
G. Dresselhaus	Bitter Magnet Lab, MIT, USA
M. Zheng	DuPont, USA
A. K. Swan	Comp. & Elec. Eng., BU, USA
B. B. Goldberg	Physics, BU, USA
S. M. Unlu	Comp. & Elec. Eng., BU, USA
M. Pimenta	Physics, UFMG, Brazil
H. B. Ribeiro	Physics, UFMG, Brazil
C. Fantini	Physics, UFMG, Brazil
F. Plentz	Physics, UFMG, Brazil
A. P. Santos	CDTN, Brazil
M. Terrones	San Luis Potosi, Mexico